European Journal of Medicinal Chemistry 89 (2015) 581–596

Contents lists available at ScienceDirect

European Journal of Medicinal Chemistry

journal homepage: http://www.elsevier.com/locate/ejmech

Original article

Design, synthesis and biological evaluation of bis-aryl ureas and amides based on 2-amino-3-purinylpyridine scaffold as DFG-out B-Raf kinase inhibitors

Weimin Yang [a], Yadong Chen [a], Xiang Zhou [a], Yazhou Gu [a], Wenqi Qian [a], Fan Zhang [a], Wei Han [a], Tao Lu [a, b, *], Weifang Tang [a, **]

[a] School of Basic Sciences, China Pharmaceutical University, 639 Longmian Avenue, Nanjing, Jiangsu 211198, China
[b] State Key Laboratory of Natural Medicines, China Pharmaceutical University, 24 Tongjiaxiang, Nanjing, Jiangsu 210009, China

ARTICLE INFO

Article history:
Received 17 March 2014
Received in revised form
14 October 2014
Accepted 14 October 2014
Available online 16 October 2014

Keywords:
B-Raf inhibitors
DFG-Out
Melanoma
Antitumor agents

ABSTRACT

By combining the scaffolds of UI-125 and Sorafenib, a series of bis-aryl ureas and amides based on 2-amino-3-purinylpyridine moiety were designed and synthesized as novel DFG-out B-Raf^{V600E} inhibitors. Among them, **20c**–**e**, **20g** and **21h** displayed potent antiproliferative activities against melanoma A375 (B-Raf^{V600E}) cell lines with IC_{50} values of 3.190, 2.276, 1.856, 1.632 μM and 1.839 μM, respectively, comparable with the positive control Vemurafenib (IC_{50} = 3.32 μM). Selected compounds were tested for the ERK inhibition in human melanoma A375 (B-Raf^{V600E}) and SK-MEL-2 (B-Raf^{WT}) cell lines by Western blot. The results revealed that our compounds inhibited the proliferation of melanoma A375 cells (B-Raf^{V600E}) through ERK pathway, without paradoxical activation of ERK in melanoma SK-MEL-2 cells (B-Raf^{WT}). Eventually, **20g** and **21h** were selected to confirm their inhibitory effects on tumor growth in A375 xenograft models in mice. Compound **20g** exhibited equivalent antitumor efficacy *in vivo* (T/C = 44.37%), compared to Sorafenib (T/C = 37.35%), by 23-day repetitive administration of a single dose of 50 mg/kg without significant body weight loss.

1. Introduction

As significant players of the conserved MAPK cascade (Ras–Raf–MEK–ERK signaling pathway), Raf kinases including A-Raf, B-Raf and C-Raf (Raf-1), are critical in mediating cell proliferation and survival [1]. B-Raf displays more potential biochemical activity than A-Raf and Raf-1 [2]. Furthermore, over 40 different mutations in B-Raf kinase domain have been identified to date, in contrast to rare mutations found in A-Raf and Raf-1 [2]. Over 90% of aberration in B-Raf is a substitution of a glutamic acid for valine at residue 600 (V600E) [3], which is particularly associated with melanoma and occurs with a frequency of 60% [4]. Based on epidemiology and preclinical target conformation, B-Raf has been recognized as an attractive target for cancer treatment [5].

Accumulating compounds have been developed as antitumor agents targeting B-Raf and categorized into two types: DFG-in and DFG-out, according to their binding modes derived from crystallographic analysis and molecular modeling [2,6,7]. The DFG-in inhibitors, such as Vemurafenib (**1**) and Dabrafenib (**2**), bind to the ATP binding site of the kinase with a DFG-in "active" conformation and exhibit potential and highly selective inhibition against B-Raf^{V600E} (Fig. 1). The DFG-out inhibitors such as Sorafenib (**3**) and RAF265 (**4**), engage the protein stable in DFG-out conformation (Fig. 1). Recently, the rapid development of secondary malignancies is reported as a well-known side effect among those selective B-Raf^{V600E} inhibitors [8–12] due to the paradoxical stimulation of MAPK signaling in cells bearing wild-type B-Raf (B-Raf^{WT}) and Raf-1 [13,14]. It is demonstrated that the feedback activation in B-Raf^{WT} bearing cancers can be significantly suppressed by DFG-out Raf inhibitors, but not by DFG-in type [15]. Hence, an optimal B-Raf inhibitor should be DFG-out type that preserves potency against oncogenic B-Raf without driving hyperactivation of B-Raf^{WT} or Raf-1.

UI-152 (**5**, Fig. 2) has been disclosed as a potent and selective ATP-competitive B-Raf inhibitor with an IC_{50} value of 1 nM [16]. Like other oncogenic B-Raf inhibitors, UI-152 has also been

* Corresponding author. State Key Laboratory of Natural Medicines, China Pharmaceutical University, 24 Tongjiaxiang, Nanjing, Jiangsu 210009, China.
** Corresponding author.
E-mail addresses: lutao@cpu.edu.cn, lut163@163.com (T. Lu), twf@cpu.edu.cn (W. Tang).

http://dx.doi.org/10.1016/j.ejmech.2014.10.039
0223-5234/

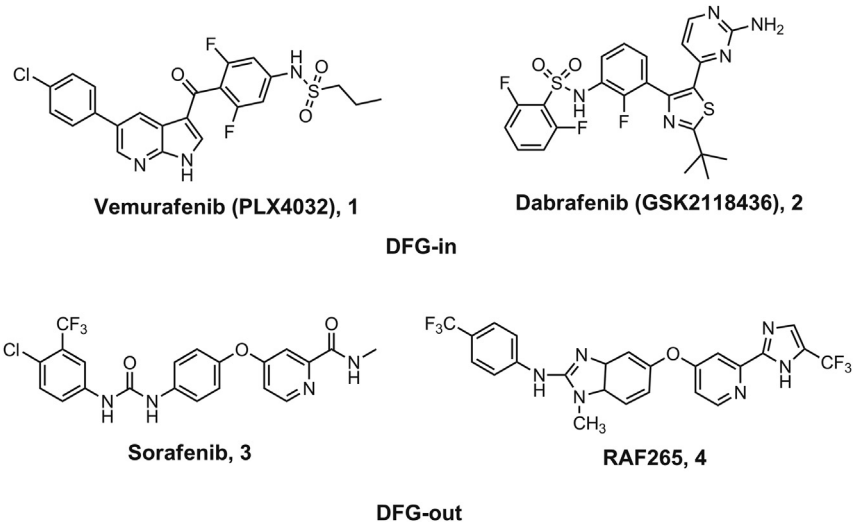

Fig. 1. Structures of Vemurafenib (**1**), Dabrafenib (**2**), Sorafenib (**3**) and RAF265 (**4**).

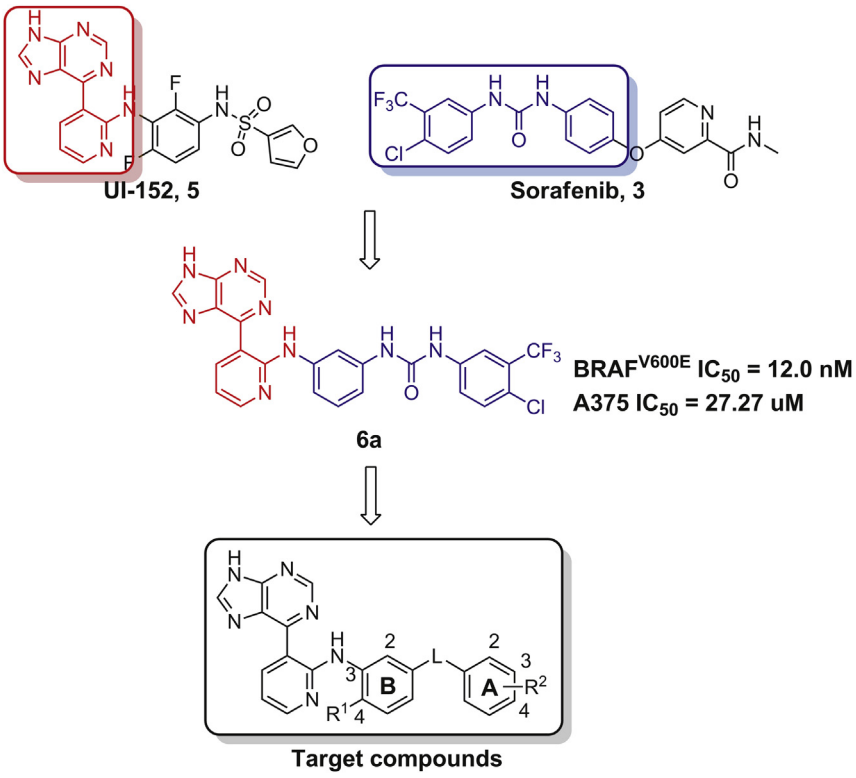

Fig. 2. Chemical structures of **UI-152**, compound **6a** and target compounds.

reported to cause the paradoxical activation of the MAPK pathway through activating phosphorylation of downstream ERK kinase in B-Raf^{WT} bearing cancers [16]. Our current work demonstrated that a novel DFG-out inhibitor **6a** could be evolved from UI-152 by replacing the furan-3-sulfonamide moiety with bis-aryl urea fragment, while remaining the 2-amino-3-purinylpyridine core intact (Fig. 2). Subsequent optimization of **6a** focused on the ring A–linker–ring B domain and provided a series of 2-amino-3-purinylpyridine scaffold based derivatives for further biological evaluation and structure–activity relationship (SAR) exploration (Fig. 2). Downstream inhibitions of ERK phosphorylation (p-ERK) were performed in both B-Raf^{V600E} mutant and B-Raf^{WT} harboring melanoma cells lines. *In vivo* studies in a human melanoma A375 xenograft model were also investigated in our work.

2. Results and discussion

2.1. Inhibitors design and molecular modeling

6a was employed as a starting point for further optimization to develop more attractive and potent compounds. We first changed the linker between phenyl ring A and B from urea (NHCONH) to

amide (NHCO) and "reverse" amide (CONH) based upon the previously known B-Raf inhibitor designs [17–19]. Then the replacement of R^1 at C-4 position on phenyl ring B with different lipophilic groups was attempted to investigate their effects on kinase activity (Fig. 3). Finally, the terminal phenyl ring A was substituted with a variety of other functionalities for further optimization. A two-dimensional pharmacophore map depicted the interaction between our compounds and B-Raf^{V600E} in a simplified form shown in Fig. 3. From this pharmacophore model, we can speculate that: (1) the purine ring is significant to form hydrogen bonds with Cys532 of the hinge region; (2) either urea or amide as linkers form the required hydrogen bonds with the conserved Glu501 of the αC-helix and the backbone amide of Asp594 from the DFG motif; (3) R^1 group on phenyl ring B occupies a small hydrophobic pocket typically closed off the gatekeeper region; (4) the R^2 substituted phenyl ring A is exposed to the hydrophobic back pocket which is made accessible by a rearrangement of the activation loop and subsequent movement of a phenylalanine side chain of DFG loop [20]. Based on these information, a library of 25 novel inhibitors were designed and then synthesized.

2.2. Chemistry

A total of 25 important intermediates of anilines **9a**–**b**, **13a**–**o** and **16a**–**h** were synthesized according to Scheme 1 via a two-step process. Urea analogs **8a** and **8b** were generated from 4-methyl-3-nitroaniline (**7a**) and 3-nitroaniline (**7b**) with 1-chloro-4-isocyanato-2-(trifluoromethyl)benzene, while amide analogs **12a**–**o** and **15a**–**h** were obtained by condensation of benzoic acid **10a**–**d** and **14a**–**g** with their corresponding anilines **11a**–**j** and **7a**–**b** listed in Scheme 1. The amide-forming reactions were carried out in the presence of EDCI and HOBt in anhydrous DMF at the room temperature for 4–24 h. Then, reduction of the nitro group for **8a**–**b**, **12a**–**o** and **15a**–**h** was carried out by using 5% Pd/C in ethanol/tetrahydrofuran (1:1) under hydrogenation conditions at the room temperature for about 3–6 h to generate the aniline products **9a**–**b**, **13a**–**o** and **16a**–**h**.

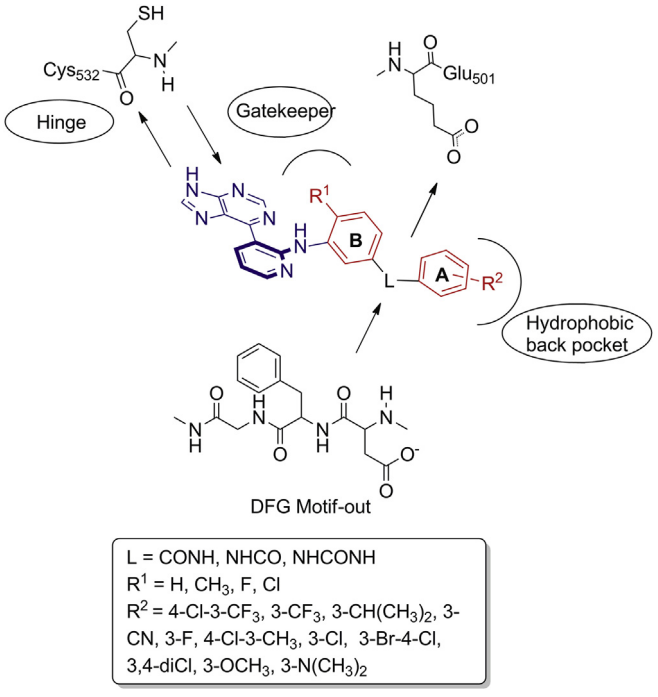

Fig. 3. Structural modification of 2-amino-3-purinylpyridine derivatives and the two-dimensional pharmacophore map of binding mode to the DFG-out conformation of B-Raf.

The synthetic route of target compounds **6a**–**b**, **20a**–**o** and **21a**–**h** is outlined in Scheme 2. The commercially available 6-chloro-9*H*-purine **17** was converted to 6-chloro-9-(tetrahydro-2*H*-pyran-2-yl)-9*H*-purine **18** according to a reported method with minor modification [21]. Subsequently, the reaction of **18** with 2-fluoro-3-pyridylboronic acid through a Suzuki–Miyaura coupling provided **19** [22]. Then, **19** were converted to **6a**–**b**, **20a**–**o** and **21a**–**h** through SN_{Ar} reaction with the previously prepared different substituted amines **9a**–**b**, **13a**–**o** and **16a**–**h** (Scheme 2) using lithium bis(trimethylsilyl)amide (LiHMDS) as a base in tetrahydrofuran (THF) in reflux condition, followed by removal of the THP protecting group under acidic conditions to afford target compounds **6a**–**b**, **20a**–**o** and **21a**–**h**.

2.3. Biological evaluation

2.3.1. B-Raf^{V600E} inhibitory assay

The newly synthesized compounds were evaluated as B-Raf^{V600E} inhibitors using Sorafenib and Vemurafenib as positive reference compounds. As shown in Table 1, all compounds showed superior potency to Sorafenib (IC_{50} = 26.4 nM) and Vemurafenib (IC_{50} = 23.0 nM) with IC_{50} values at nanomolar ranges. Particularly, compounds **20e** (IC_{50} = 0.717 nM), **21d** (IC_{50} = 0.669 nM) and **21h** (IC_{50} = 0.790 nM) showed remarkable potency with IC_{50} values less than 1 nM.

2.3.2. Antiproliferative assay against A375 cells in vitro

As described above, B-Raf^{V600E} was an important target for developing small-molecular inhibitors for cancer therapies, especially melanoma. The antiproliferative activities of all synthesized compounds against A375 cells (B-Raf^{V600E}) were evaluated and the results were summarized in Table 1. Compounds **20c**–**e**, **20g** and **21h** (IC_{50} = 3.190, 2.276, 1.856, 1.632 μM and 1.839 μM, respectively) displayed potent antiproliferative activities against A375 cell line, comparable with the positive control Vemurafenib (IC_{50} = 3.315 μM). Almost half of the compounds proved to be superior to Sorafenib (IC_{50} = 13.64 μM) but less potent than Vemurafenib. The rest of tested compounds showed weak B-Raf inhibition with IC_{50} values range of 16.01–79.50 μM.

2.3.3. Structure–activity relationship exploration

All synthesized compounds showed distinct enzymatic and cellular inhibition due to the difference of R^1, R^2 and linker types (L) between two phenyl rings.

2.3.3.1. SAR of linker types (L) between the phenyl ring A and B. Replacement of the urea linker of **6a** with amide and "reverse" amide afforded compounds **20a** (L = NHCO) and **21a** (L = CONH), respectively. Compared to **6a** (B-Raf^{V600E} IC_{50} = 12.0 nM, A375 IC_{50} = 27.27 μM), **20a** (B-Raf^{V600E} IC_{50} = 13.5 nM, A375 IC_{50} = 61.35 μM) got a slight loss in inhibitory potency and a significantly reduced cellular activity, while **21a** (B-Raf^{V600E} IC_{50} = 3.03 nM, A375 IC_{50} = 16.01 μM) exhibited a 4-fold enhancement in B-Raf^{V600E} inhibition with attendant improvement in cellular potency. However, the methyl substituted amide **20b** (B-Raf^{V600E} IC_{50} = 3.15 nM, A375 IC_{50} = 8.785 μM) and "reverse" amide **21b** (B-Raf^{V600E} IC_{50} = 2.71 nM, A375 IC_{50} = 8.42 μM) were more potent than the corresponding urea analog **6b** (B-Raf^{V600E} IC_{50} = 4.21 nM, A375 IC_{50} = 29.73 μM) in both B-Raf^{V600E} and A375 inhibition. These results suggested that both amide (L = NHCO) and "reverse" amide (L = CONH) were tolerant to the potency. They could be both attributed to hydrogen bond formation at the specific receptor sites like the urea linker as we

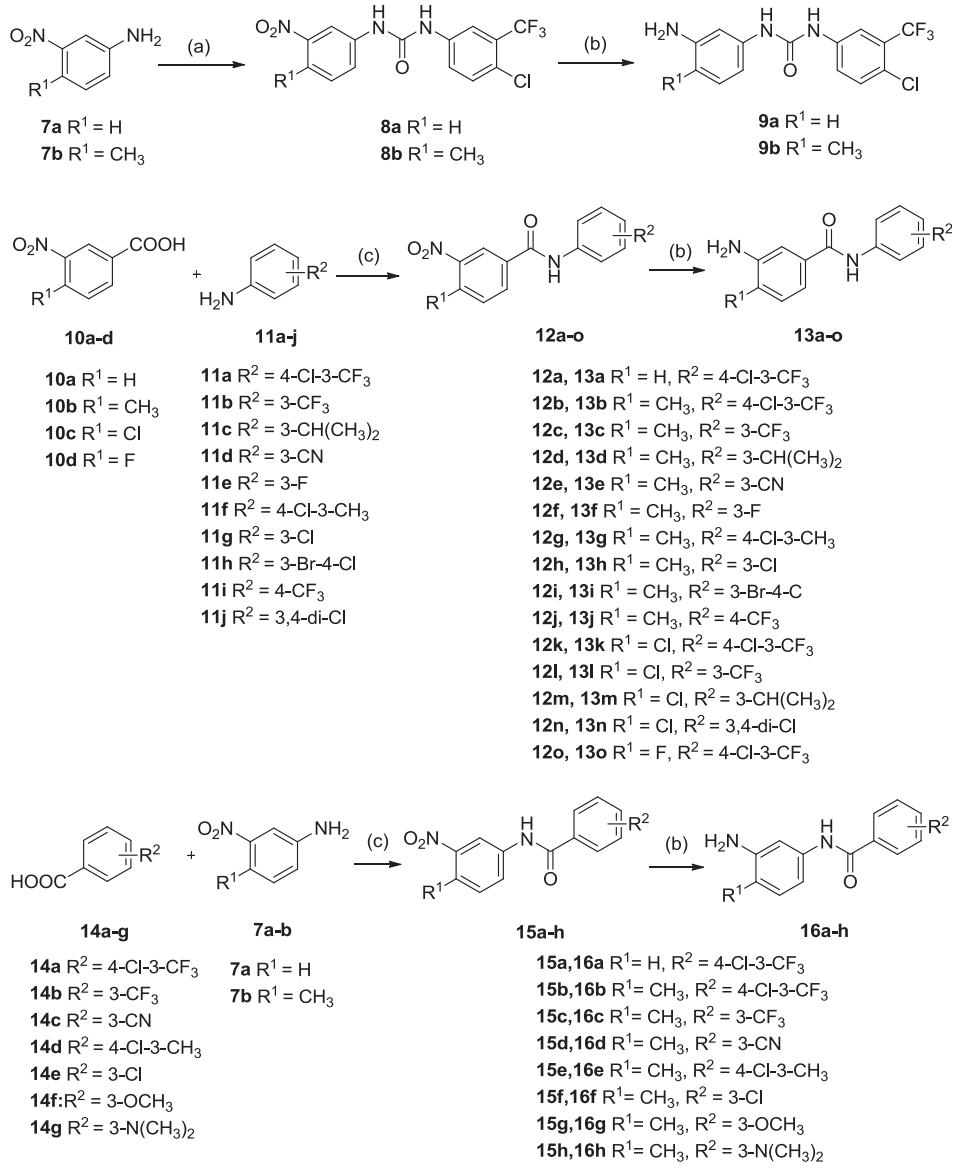

Scheme 1. The synthesis of aniline intermediates **9a**–**b**, **13a**–**o** and **16a**–**h**. *Reagents and conditions*: (a) 1-chloro-4-isocyanato-2-(trifluoromethyl)benzene, CH_2Cl_2, rt, 2 h; (b) H_2, 5% Pd/C, EtOH/THF (1:1), rt, 3–6 h; (c) EDCI, HOBt, Et_3N, DMF, rt, 4–24 h.

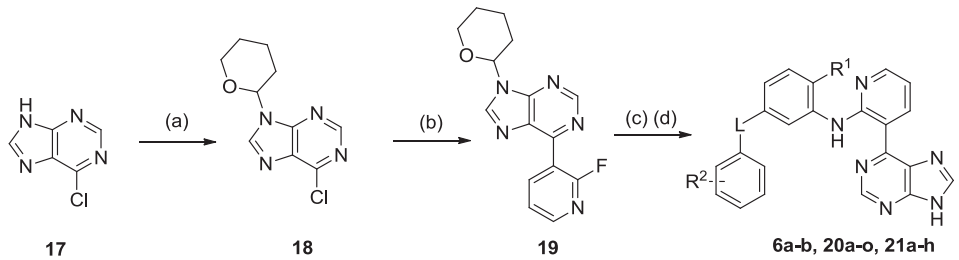

Scheme 2. Synthesis of target compounds **6a**–**b**, **20a**–**o** and **21a**–**h**. *Reagents and conditions*: (a) 3,4-dihydro-2*H*-pyran, TsOH, anhydrous EtOAc, reflux, 3 h; (b) (2-fluoropyridin-3-yl)boronic acid, $PdCl_2$(dppf), Na_2CO_3, 1,4-dioxane/H_2O (4:1), nitrogen atmosphere, reflux, 14 h; (c) **9a**–**b**, **13a**–**o** and **16a**–**h**, LiHMDS, anhydrous THF, nitrogen atmosphere, rt, 2–6 h; (d) 1 N HCl, MeOH, rt, 2 h.

estimated (Fig. 3). Further evaluation of **20b**–**j** and **21b**–**h** revealed that the amide derivatives (L = NHCO) shared fairly comparable potency with "reverse" amide analogs (L = CONH) against B-Raf^{V600E} and A375 cells.

2.3.3.2. SAR of substitutions R^1 on the ring B. Subsequently, the influence of R^1 substituent at C-4 position on ring B was probed. Compounds **6b**, **20b** and **21b** with methyl substitution displayed enhanced B-Raf kinase inhibition, as well as A375 antiproliferative

Table 1
The list of bis-aryl urea and amide analogs based on 2-amino-3-purinylpyridine scaffold and biological evaluation against B-Raf and melanoma A375 cells.

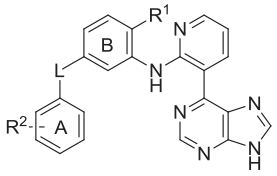

Compounds	L	R^1	R^2	IC_{50} values	
				B-Raf[a] (nM)	A375[b,c] (μM)
6a	NHCONH	H	4-Cl-3-CF_3	12.0	27.27 ± 17.055
6b	NHCONH	CH_3	4-Cl-3-CF_3	4.21	29.73 ± 6.89
20a	NHCO	H	4-Cl-3-CF_3	13.5	61.35 ± 39.71
20b	NHCO	CH_3	4-Cl-3-CF_3	3.15	8.785 ± 2.300
20c	NHCO	CH_3	3-CF_3	2.17	3.190 ± 0.751
20d	NHCO	CH_3	3-$CH(CH_3)_2$	1.69	2.276 ± 0.773
20e	NHCO	CH_3	3-CN	0.717	1.856 ± 0.47
20f	NHCO	CH_3	3-F	1.03	79.50 ± 55.27
20g	NHCO	CH_3	4-Cl-3-CH_3	1.43	1.632 ± 0.482
20h	NHCO	CH_3	3-Cl	1.30	6.285 ± 1.6
20i	NHCO	CH_3	3-Br-4-Cl	3.62	10.01 ± 3.054
20j	NHCO	CH_3	4-CF_3	1.50	10.03 ± 2.11
20k	NHCO	Cl	4-Cl-3-CF_3	10.8	13.28 ± 4.212
20l	NHCO	Cl	3-CF_3	2.78	11.43 ± 3.242
20m	NHCO	Cl	3-$CH(CH_3)_2$	8.07	7.512 ± 1.444
20n	NHCO	Cl	3,4-di-Cl	1.60	51.95 ± 30.325
20o	NHCO	F	4-Cl-3-CF_3	4.82	19.97 ± 3.98
21a	CONH	H	4-Cl-3-CF_3	3.03	16.01 ± 3.96
21b	CONH	CH_3	4-Cl-3-CF_3	2.71	8.42 ± 1.898
21c	CONH	CH_3	3-CF_3	2.51	7.17 ± 1.493
21d	CONH	CH_3	3-CN	0.669	10.62 ± 3.279
21e	CONH	CH_3	4-Cl-3-CH_3	2.56	6.914 ± 1.761
21f	CONH	CH_3	3-Cl	1.77	10.75 ± 2.866
21g	CONH	CH_3	3-OCH_3	1.20	3.718 ± 1.19
21h	CONH	CH_3	3-$N(CH_3)_2$	0.790	1.839 ± 0.572
22	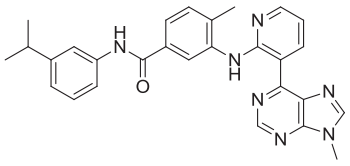			7.44	68.83 ± 33.68
23	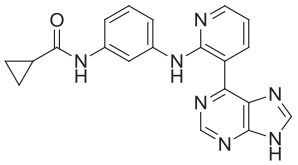			471	>100
24	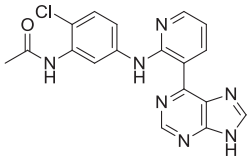			6430	>100
Sorafenib				26.4	13.64 ± 3.045
Vemurafenib				23.0	3.315 ± 0.58

[a] B-Raf^{V600E} inhibitory assay.
[b] Antiproliferative assay in A375 cells.
[c] Values are expressed as means ± SD (standard deviation) of five experiments.

potency than the corresponding unsubstituted compounds **6a**, **20b** and **21b**. The comparison indicated that the methyl group in R^1 position was beneficial for the potency. This result was consistent with the hypothesis that the R^1 group would occupy a small hydrophobic pocket typically closed off the gatekeeper region in B-Raf. Furthermore, halogen atoms, including fluorine and chloride, were also employed to afford compounds **20k**–**o**. However, these halogen-substituted compounds displayed obviously less inhibitory performances than the methyl substituted derivatives **20b**–**d**. The strength order against B-Raf^{V600E} is CH_3 > F > Cl > H, while the potency order against A375 is CH_3 > Cl > F > H. These results proved that C-4 substitution of methyl group on phenyl ring B was a fruitful

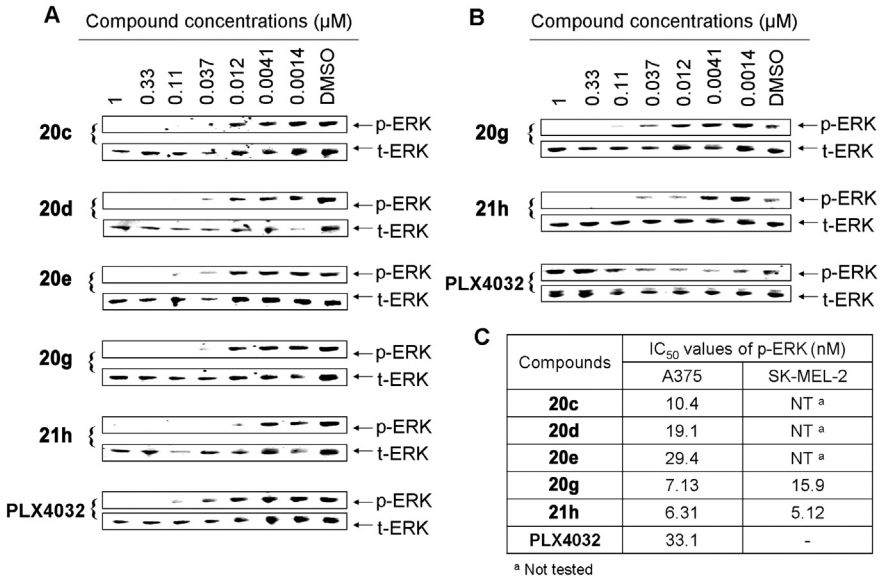

C

Compounds	IC_{50} values of p-ERK (nM)	
	A375	SK-MEL-2
20c	10.4	NT [a]
20d	19.1	NT [a]
20e	29.4	NT [a]
20g	7.13	15.9
21h	6.31	5.12
PLX4032	33.1	-

[a] Not tested

Fig. 4. Compounds **20c**–**e**, **20g** and **21h** potently inhibits ERK phosphorylation. A375 (A) or SK-MEL-2 (B) human malignant melanoma cells were treated with the indicated concentrations of our compounds or reference compound PLX4032 (starting at 1 μM, 7 doses, 3 fold dilution) for 90 min. The ERK phosphorylation (p-ERK) and expression levels (t-ERK) were analyzed by Western blotting with anti-phospho-ERK antibody or anti-ERK antibody. (C) Summary of the IC_{50} values by Western blot assay.

approach to enhance B-Raf^{V600E} inhibition relative to melanoma A375 cells antiproliferative activity.

2.3.3.3. SAR of substitutions R^2 on the ring A. Different lipophilic substitutions were attempted at the *meta* and (or) *para* positions of terminal phenyl ring A (R^2) to determine their effects on potency, affording derivatives **20c**–**j** and **21c**–**h**. Apart from 4-chloro-3-bromo substituent found in compounds **20i**, both electron withdrawing groups (like halogen, cyano) and electron donating groups (like methoxy, dimethylamino) were more accommodated than the initial 4-chloro-3-trifluoromethyl group. Compounds **20e** (IC_{50} = 0.717 nM), **21d** (IC_{50} = 0.669 nM) and **21h** (IC_{50} = 0.790 nM) disclosed the best kinase inhibition with IC_{50} values less than 1 nM, while compounds **20c**–**e**, **20g** and **21h** exhibited the highest potency against human melanoma A375 cell line with IC_{50} values of 3.190, 2.276, 1.856, 1.632 μM and 1.839 μM, respectively. These results suggested that 3-trifluromethyl, 3-isopropyl, 3-cyano, 4-chloro-3-methyl and 3-dimethylamino groups were beneficial for potency. However, 3-fluro group found in compound **20f** (B-Raf^{V600E} IC_{50} = 1.03 nM, A375 IC_{50} = 79.50 μM) was unfavorable due to the 9-fold reduction of antiproliferative potency, compared with **20b** (A375 IC_{50} = 8.785 μM).

2.3.3.4. SAR of purine ring and terminal phenyl ring A. A methyl group was added onto the 9-N*H* of purine ring of **20d** (B-Raf^{V600E} IC_{50} = 1.69 nM, A375 IC_{50} = 2.276 μM), affording compound **23** (B-Raf^{V600E} IC_{50} = 7.44 nM, A375 IC_{50} = 68.83 μM), which resulted in a 34-fold loss of antiproliferative activity (Table 1). The synthetic route and procedure of compound **22** were listed in Supplementary data. This result confirmed that the 9-N*H* on purine ring was significant to remain the hydrogen bond interactions with hinge residues of B-Raf^{V600E}. Meanwhile, terminal aromatic ring A were replaced into non-aromatic fragments such as cyclopropyl ring and methyl group to generate compound **23** (B-Raf^{V600E} IC_{50} = 471 nM, A375 IC_{50} > 100 μM) and **24** (B-Raf^{V600E} IC_{50} = 6.43 μM, A375 IC_{50} > 100 μM), respectively. They were also synthesized (listed in Supplementary data) and evaluated, but almost inactive in both kinase and cellular inhibition (Table 1). The bis-aryl ring structure is estimated significant for the potency and the binding affinity between the terminal phenyl ring A and the hydrophobic pocket.

2.3.4. ERK kinase inhibition in A375 cells

In order to explore the biological mechanism of these DFG-out compounds, **20c**–**e**, **20g** and **21h** with high potency against human melanoma A375 cell line were selected as representative examples to be tested for their inhibitory effects on ERK kinases using reported Western blot methods [15,23,24]. A375 cell lysate was treated with seven different concentrations (1 μM as starting concentration with 3 fold dilution) of the test compounds, and their inhibitory activities were compared with that of Vemurafenib (PLX4032). The results displayed as Western blot band signals in Fig. 4A, indicating that our compounds and Vemurafenib markedly suppressed phosphorylation of ERK1/2 in a dose dependent manner. Furthermore, the IC_{50} values of ERK phosphorylation in A375 cells of these five compounds was listed in Fig. 4C, suggesting that all compounds exhibited much more strong inhibitory effects quantitatively on the ERK kinase than Vemurafenib. Therefore, the result validated the hypothesis that these compounds may inhibit the proliferation of melanoma cells harboring B-Raf^{V600E} mutation through ERK pathway. The observed activities were not due to off-target effects on proliferation but B-Raf inhibition.

2.3.5. ERK kinase inhibition in SK-MEL-2 cells

Reflecting the potent B-Raf^{V600E} inhibitory activities *in vitro*, compounds **20g** and **21h** inhibited phosphorylation of ERK (p-ERK) in melanoma A375 cells with IC_{50} values of 7.13 nM and 6.31 nM, respectively (Fig. 4C). Subsequently, the inhibition of ERK phosphorylation (p-ERK) were also evaluated against melanoma SK-MEL-2 cells expressing B-Raf^{WT}, which have been reported to be insensitive to selective B-Raf^{V600E} inhibitors such as Vemurafenib. The results displayed as Western blot band signals in Fig. 4B. Vemurafenib was observed to activate the signal transduction of the MAPK cascade through phosphorylation of ERK in a dose-dependent manner in SK-MEL-2 cells. However, compounds **20g** and **21h** were assessed to inhibit the phosphorylation of ERK (p-ERK) potently with IC_{50} values of 15.9 nM and 5.12 nM, respectively (Fig. 4C). These results showed that the bis-aryl ureas and amides

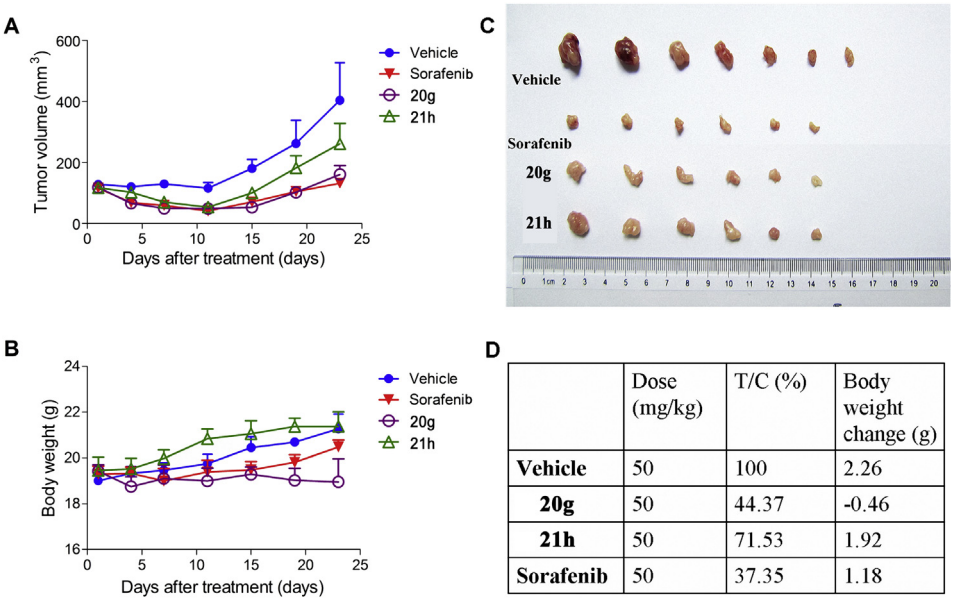

D

	Dose (mg/kg)	T/C (%)	Body weight change (g)
Vehicle	50	100	2.26
20g	50	44.37	-0.46
21h	50	71.53	1.92
Sorafenib	50	37.35	1.18

Fig. 5. Antitumor activities of **20g** and **21h** (i.g.) in human melanoma A375 (B-Raf^{V600E}) bearing Balb/c-nu nude mice (A) Mean with SEM values ($n = 6$; $^*P \leq 0.05$ *vs* Vehicle) of tumor volumes according to days after the treatment of Sorafenib, **20g**, **21h** and vehicle group. (B) Mean with SEM values ($n = 6$; $^*P \leq 0.05$ *vs* Vehicle) of body weight according to days after the treatment of Sorafenib, **20g**, **21h** and vehicle group. (C) The photograph of tumors from dissected mice at the end of experiment. (D) Summary of doses, T/C values and body weight changes in A375 (B-Raf^{V600E}) xenograft models.

based on 2-amino-3-purinylpyridine moiety would apparently suppress the proliferation of B-Raf^{V600E} positive melanoma cell lines without activation of the MAPK signaling in B-Raf^{WT} bearing cells. The most representative compounds **20g** and **21h** could be identified as promising antitumor agents to treat melanoma patients with either B-Raf^{V600E} or B-Raf^{WT}.

2.3.6. *In vivo studies of compounds **20g** and **21h** in Balb/c-nu nude mice*

To preliminarily examine the efficacy of **20g** and **21h** *in vivo*, the two compounds were prepared in solid dispersion (SD) formulation and intragastrically administered once daily for 23 days over a single dose of 50 mg/kg in a human melanoma A375 (B-Raf^{V600E}) xenograft model in Balb/c-nu nude mice (Fig. 5). As a result, compound **21h** displayed obvious antitumor efficacy (T/C = 71.53%) compared with the vehicle control and showed no signs of body weight loss (body weight change: +1.92 g) (Fig. 5D). In particular, compound **20g** exhibited equivalent similar antitumor efficacy (T/C = 44.37%) in comparison with the positive control drug Sorafenib (T/C = 37.35%) without severe body weight reduction (body weight change: −0.46 g) (Fig. 5D).

3. Conclusion

The bis-aryl urea derivative **6a** as a novel and potent DFG-out B-Raf^{V600E} inhibitor was evolved from a scaffold combination of UI-125 and Sorafenib. Subsequent optimization of the ring A−linker−ring B domain provided a class of bis-aryl amides based on 2-amino-3-purinylpyridine moiety. All synthesized compounds were evaluated for B-Raf^{V600E} kinase inhibition, as well as melanoma A375 antiproliferative potency. The SAR study indicated that the methyl substitution at C-4 position on the ring B, amides as linkers between the phenyl rings and lipophilic groups at *meta* or *para* position on ring A are beneficial for improving potency. All compounds exhibited potent B-Raf^{V600E} inhibition with IC_{50} values ranging from 0.70 to 13.5 nM, comparing to Vemurafenib (IC_{50} = 23.0 nM). Compounds **20c**–**e**, **20g** and **21h** displaying potent antiproliferative activities against A375 cell line with IC_{50} values of 3.190, 2.276, 1.856, 1.632 μM and 1.839 μM, respectively, were selected for further evaluation of the p-ERK inhibition in human melanoma A375 (B-Raf^{V600E}) and SK-MEL-2 (B-Raf^{WT}) cells. A key finding from this class of compounds was that, unlike PLX4032, they dramatically inhibited the proliferation of melanoma A375 cells (B-Raf^{V600E}) through ERK pathway, without paradoxical activation of the MAPK in SK-MEL-2 (B-Raf^{WT}) cells. The most potent compounds **20g** and **21h** were progressed to *in vivo* profiling. **20g** exhibited similarly equivalent tumor growth inhibition (T/C = 44.37%) by contrast to Sorafenib (T/C = 37.35%) with no significant body weight loss. The further study will focus on the physicochemical property improvement and druggabilityoptimization of these compounds, for the poor water-solubility was observed during the pharmacological experiments, which is supposed to dramatically affect the inhibition of tumor growth *in vivo*.

4. Experimental protocols

4.1. Chemistry

All starting materials were obtained from commercial suppliers and used without further purification. NMR spectra were recorded, on a Bruker DPX-300 spectrometer, in DMSO-d_6 or $CDCl_3$-d_6 using TMS as the internal standard. Chemical shifts (δ) were reported in parts per million downfield from the internal standard. The signals were quoted as s (singlet), d (doublet), t (triplet), m (multiplet). Analytical thin-layer chromatography (TLC) was performed with silica gel 60 F_{254}, 0.25 mm per-coated TLC plates. TLC plates were visualized using UV_{254}. Column chromatography was conducted on silica gel (230–400 mesh). Mass spectra were obtained on a Waters Quattro Micromass instrument using electrospray ionization (ESI) technique.

4.1.1. *General procedure for the preparation of 3-nitrobisaryl ureas (**8a**, **8b**)*

1-Chloro-4-isocyanato-2-(trifluoromethyl)benzene (5 mmol) was added to a solution of **7a** or **7b** (5 mmol) in anhydrous

dichloromethane at room temperature. As the mixture was stirred for 2 h, pure solid appeared in the solvent. After completion of the reaction as indicated by TLC, precipitated product was collected by filtration, washed well with dichloromethane and dried to provide the intermediates **8a**, **8b**.

*4.1.1.1. 1-(4-Chloro-3-(trifluoromethyl)phenyl)-3-(3-nitrophenyl) urea (**8a**).* Light yellow solid (1.58 g, 88.0%) was obtained from **7a**. Mp: 229–231 °C. ESI-MS *m/z*: 359.0 $[M+H]^+$. ^{1}H NMR (300 MHz, DMSO-d_6): δ 7.68–7.88 (5H, m, H–Ar), 8.12 (1H, s, H–Ar), 8.54 (1H, d, H–Ar, J = 1.8 Hz), 9.38 (1H, s, *NH*CONH), 9.44 (1H, s, NHCO*NH*).

*4.1.1.2. 1-(4-Chloro-3-(trifluoromethyl)phenyl)-3-(4-methyl-3-nitrophenyl)urea (**8b**).* Light yellow solid (1.64 g, 87.6%) was obtained from **7b**. Mp: 219–220 °C. ESI-MS *m/z*: 373.0 $[M+H]^+$. ^{1}H NMR (300 MHz, DMSO-d_6): δ 2.46 (3H, s, $ArCH_3$), 7.42 (1H, d, H–Ar, J = 8.4 Hz), 7.58–7.69 (3H, m, H–Ar), 8.11 (1H, d, H–Ar, J = 2.1 Hz), 8.28 (1H, d, H–Ar, J = 2.1 Hz), 9.26 (1H, s, *NH*CONH), 9.31 (1H, s, NHCO*NH*).

*4.1.2. General procedure for the preparation of 3-nitrobenzamide and N-3-nitrobenzamide analogs (**12a**–**o**, **15a**–**h**)*

A mixture of 4-substituted-3-nitrobenzoic acid **10a**–**d**, **14a**–**g** (5 mmol), EDCI (6 mmol) and HOBt in anhydrous DMF (20 mL) was stirred at room temperature for about 0.5–2 h. Then the appropriate aniline **11a**–**j**, **7a**–**b** (4 mmol) was added with triethylamine (5 mmol) and stirred at room temperature for 4–24 h. Then the reaction mixture was diluted to 100 mL with water and extracted with EtOAc (3 × 30 mL). The combined organic layers were washed with saturated solution of NaCl, then dried over $MgSO_4$ and concentrated under reduced pressure. The residue was chromatographed over silica gel column using acetic ether and petroleum ether (1:10–1:8, v:v) as eluent to obtain compounds **12a**–**o**, **15a**–**h** as white solid.

*4.1.2.1. N-(4-chloro-3-(trifluoromethyl)phenyl)-3-nitrobenzamide (**12a**).* White-off solid (1.03 g, 74.5%) was obtained from **10a** and **11a**. Mp: 189–190 °C. ESI-MS *m/z*: 345.0 $[M+H]^+$. ^{1}H NMR (300 MHz, DMSO-d_6): δ 7.76 (1H, d, H–Ar, J = 8.7 Hz), 7.88 (1H, t, H–Ar, J = 8.1 Hz), 8.13 (1H, dd, H–Ar, J = 2.1 Hz, J = 8.7 Hz), 8.36 (1H, d, H–Ar, J = 2.1 Hz), 8.42 (1H, d, H–Ar, J = 2.1 Hz), 8.48 (1H, dd, H–Ar, J = 1.8 Hz, J = 8.1 Hz), 8.83 (1H, t, H–Ar, J = 1.8 Hz), 10.96 (1H, s, CONH).

*4.1.2.2. N-(4-chloro-3-(trifluoromethyl)phenyl)-4-methyl-3-nitrobenzamide (**12b**).* White solid (1.10 g, 76.9%) was obtained from **10b** and **11a**. Mp: 174–175 °C. ESI-MS *m/z*: 359.0 $[M+H]^+$. ^{1}H NMR (300 MHz, $CDCl_3$): 2.48 (3H, s, $ArCH_3$), 7.52 (1H, d, H–Ar, J = 8.7 Hz), 7.69 (1H, dd, H–Ar, J = 2.4 Hz, J = 9.0 Hz), 8.00 (1H, d, H–Ar, J = 8.7 Hz), 8.24–8.30 (2H, m, H–Ar), 8.64 (1H, d, H–Ar, J = 2.1 Hz), 10.83 (1H, s, NHCO).

*4.1.2.3. N-(3-(trifluoromethyl)phenyl)-4-methyl-3-nitrobenzamide (**12c**).* White solid (0.978 g, 75.4%) was obtained from **10b** and **11b**. Mp: 154–156 °C. ESI-MS *m/z*: 325.0 $[M+H]^+$. ^{1}H NMR (300 MHz, DMSO-d_6): 2.46 (3H, s, $ArCH_3$), 7.53 (1H, d, H–Ar, J = 8.4 Hz), 7.82 (1H, t, H–Ar, J = 7.8 Hz), 8.02 (2H, dd, H–Ar, J = 2.1 Hz, J = 8.4 Hz), 8.29 (1H, d, H–Ar, J = 7.8 Hz), 8.33 (1H, s, H–Ar), 8.54 (1H, d, H–Ar, J = 2.1 Hz), 10.84 (1H, s, NHCO).

*4.1.2.4. N-(3-isopropylphenyl)-4-methyl-3-nitrobenzamide (**12d**).* Light brown solid (0.893 g, 74.8%) was obtained from **10b** and **11c**. Mp: 102–104 °C. ESI-MS *m/z*: 299.1 $[M+H]^+$. ^{1}H NMR (300 MHz, DMSO-d_6): 1.22 (6H, d, $CH(CH_3)_2$, J = 6.9 Hz), 2.48 (3H, s, $ArCH_3$), 2.82–2.93 (1H, m, $CH(CH_3)_2$), 7.03 (1H, d, H–Ar, J = 7.5 Hz), 7.29 (1H, t, H–Ar, J = 8.4 Hz), 7.62 (2H, d, H–Ar, J = 1.8 Hz), 7.98 (1H, d, H–Ar, J = 8.4 Hz), 8.27 (1H, dd, H–Ar, J = 2.1 Hz, J = 8.4 Hz), 8.64 (1H, d, H–Ar, J = 2.1 Hz), 10.49 (1H, s, NHCO).

*4.1.2.5. N-(3-cyanophenyl)-4-methyl-3-nitrobenzamide (**12e**).* White solid (0.934 g, 83.0%) was obtained from **10b** and **11d**. Mp: 165–167 °C. ESI-MS *m/z*: 282.1 $[M+H]^+$. ^{1}H NMR (300 MHz, DMSO-d_6): 2.34 (3H, s, $ArCH_3$), 7.52 (1H, t, H–Ar, J = 8.1 Hz), 7.68 (1H, dd, H–Ar, J = 4.8 Hz, J = 8.1 Hz), 7.90 (2H, s, H–Ar), 7.70–7.76 (1H, m, H–Ar), 8.32 (1H, dd, H–Ar, J = 2.4 Hz, J = 8.9 Hz), 8.47 (1H, d, H–Ar, J = 2.1 Hz), 10.84 (1H, s, NHCO).

*4.1.2.6. N-(3-fluorophenyl)-4-methyl-3-nitrobenzamide (**12f**).* White solid (0.828 g, 75.5%) was obtained from **10b** and **11e**. Mp: 165–167 °C. ESI-MS *m/z*: 275.1 $[M+H]^+$. ^{1}H NMR (300 MHz, DMSO-d_6): 2.49 (3H, s, $ArCH_3$), 6.96–7.02 (1H, m, H–Ar), 7.39–7.46 (1H, m, H–Ar), 7.58 (1H, d, H–Ar, J = 9.0 Hz), 7.70–7.76 (1H, m, H–Ar), 8.01 (1H, d, H–Ar, J = 9.0 Hz), 8.26 (1H, dd, H–Ar, J = 2.1 Hz, J = 8.4 Hz), 8.64 (1H, d, H–Ar, J = 2.1 Hz), 10.72 (1H, s, NHCO).

*4.1.2.7. N-(4-chloro-3-methylphenyl)-4-methyl-3-nitrobenzamide (**12g**).* White solid (0.909 g, 74.6%) was obtained from **10b** and **11f**. Mp: 208–210 °C. ESI-MS *m/z*: 305.1 $[M+H]^+$. ^{1}H NMR (300 MHz, DMSO-d_6): 2.34 (3H, s, $ArCH_3$), 2.49 (3H, s, $ArCH_3$), 7.42 (1H, d, H–Ar, J = 8.7 Hz), 7.64 (1H, dd, H–Ar, J = 2.4 Hz, J = 8.7 Hz), 7.76 (1H, d, H–Ar, J = 2.1 Hz), 7.99 (1H, d, H–Ar, J = 8.4 Hz), 8.25 (1H, dd, H–Ar, J = 2.1 Hz, J = 8.4 Hz), 8.64 (1H, d, H–Ar, J = 2.1 Hz), 10.64 (1H, s, NHCO).

*4.1.2.8. N-(3-chlorophenyl)-4-methyl-3-nitrobenzamide (**12h**).* White solid (0.902 g, 77.6%) was obtained from **10b** and **11g**. Mp: 142–144 °C. ESI-MS *m/z*: 291.0 $[M+H]^+$. ^{1}H NMR (300 MHz, DMSO-d_6): 2.47 (3H, s, $ArCH_3$), 7.21 (1H, dd, H–Ar, J = 1.8 Hz, J = 7.8 Hz), 7.42 (1H, t, H–Ar, J = 8.1 Hz), 7.70 (1H, d, H–Ar, J = 8.1 Hz), 7.93–8.08 (2H, m, H–Ar), 8.26 (1H, dd, H–Ar, J = 2.1 Hz, J = 8.4 Hz), 8.64 (1H, d, H–Ar, J = 2.1 Hz), 10.69 (1H, s, NHCO).

*4.1.2.9. N-(3-bromo-4-chlorophenyl)-4-methyl-3-nitrobenzamide (**12i**).* White solid (1.24 g, 83.7%) was obtained from **10b** and **11h**. Mp: 218–220 °C. ESI-MS *m/z*: 369.0 $[M+H]^+$. ^{1}H NMR (300 MHz, DMSO-d_6): 2.46 (3H, s, $ArCH_3$), 7.69 (1H, d, H–Ar, J = 8.9 Hz), 7.79 (1H, dd, H–Ar, J = 2.4 Hz, J = 8.9 Hz), 8.01 (1H, d, H–Ar, J = 8.4 Hz), 8.24–8.30 (2H, m, H–Ar), 8.64 (1H, d, H–Ar, J = 2.1 Hz), 10.76 (1H, s, NHCO).

*4.1.2.10. N-(4-(trifluoromethyl)phenyl)-4-methyl-3-nitrobenzamide (**12j**).* White solid (1.02 g, 78.5%) was obtained from **10b** and **11i**. Mp: 145–147 °C. ESI-MS *m/z*: 325.0 $[M+H]^+$. ^{1}H NMR (300 MHz, DMSO-d_6): 2.46 (3H, s, $ArCH_3$), 7.77 (2H, d, H–Ar, J = 8.7 Hz), 8.01 (3H, d, H–Ar, J = 8.4 Hz), 8.29 (1H, dd, H–Ar, J = 2.1 Hz, J = 8.4 Hz), 8.67 (1H, d, H–Ar, J = 2.1 Hz), 10.92 (1H, s, NHCO).

*4.1.2.11. N-(4-chloro-3-(trifluoromethyl)phenyl)-4-chloro-3-nitrobenzamide (**12k**).* White solid (1.30 g, 86.1%) was obtained from **10c** and **11a**. Mp: 155–157 °C. ESI-MS *m/z*: 379.0 $[M+H]^+$. ^{1}H NMR (300 MHz, DMSO-d_6): δ 7.77 (1H, d, H–Ar, J = 8.7 Hz), 8.02 (1H, d, H–Ar, J = 8.4 Hz), 8.10 (1H, dd, H–Ar, J = 2.4 Hz, J = 8.7 Hz), 8.27 (1H, dd, H–Ar, J = 2.1 Hz, J = 8.4 Hz), 8.32 (1H, d, H–Ar, J = 2.4 Hz), 8.66 (1H, d, H–Ar, J = 2.1 Hz), 10.91 (1H, s, NHCO).

*4.1.2.12. N-(3-(trifluoromethyl)phenyl)-4-chloro-3-nitrobenzamide (**12l**).* White solid (1.10 g, 79.7%) was obtained from **10c** and **11b**. Mp: 159–160 °C. ESI-MS *m/z*: 345.0 $[M+H]^+$. ^{1}H NMR (300 MHz, $CDCl_3$): δ 7.51 (1H, d, H–Ar, J = 7.8 Hz), 7.64 (1H, t, H–Ar, J = 8.1 Hz), 8.01 (1H, d, H–Ar, J = 8.1 Hz), 8.05 (1H, d, H–Ar, J = 8.1 Hz), 8.20

(1H, s, H–Ar), 8.28 (1H, dd, H–Ar, J = 2.1 Hz, J = 8.4 Hz), 8.67 (1H, d, H–Ar, J = 2.1 Hz), 10.45 (1H, s, NHCO).

*4.1.2.13. N-(3-isopropylphenyl)-4-chloro-3-nitrobenzamide (**12m**).* White solid (1.10 g, 86.6%) was obtained from **10c** and **11c**. Mp: 144–145 °C. ESI-MS m/z: 319.1 $[M+H]^+$. ^{1}H NMR (300 MHz, DMSO-d_6): δ 1.27 (6H, d, $(CH_3)_2CH$, J = 6.9 Hz), 2.89 (1H, m, $(CH_3)_2CH$), 6.97 (1H, d, H–Ar, J = 7.5 Hz), 7.26 (1H, t, H–Ar, J = 7.8 Hz), 7.54–7.59 (2H, m, H–Ar), 7.97 (1H, d, H–Ar, J = 8.4 Hz), 8.25 (1H, dd, H–Ar, J = 2.1 Hz, J = 8.4 Hz), 8.63 (1H, d, H–Ar, J = 2.1 Hz), 10.44 (1H, s, NHCO).

*4.1.2.14. N-(3,4-dichlorophenyl)-4-chloro-3-nitrobenzamide (**12n**).* White solid (1.19 g, 81.2%) was obtained from **10c** and **11j**. Mp: 197–198 °C. ESI-MS m/z: 345.0 $[M+H]^+$. ^{1}H NMR (300 MHz, DMSO-d_6): δ 7.68 (1H, d, H–Ar, J = 8.7 Hz), 7.76 (1H, dd, H–Ar, J = 2.4 Hz, J = 8.7 Hz), 8.02 (1H, d, H–Ar, J = 8.4 Hz), 8.15 (1H, d, H–Ar, J = 2.4 Hz), 8.28 (1H, dd, H–Ar, J = 2.1 Hz, J = 8.4 Hz), 8.66 (1H, d, H–Ar, J = 2.1 Hz), 10.80 (1H, s, NHCO).

*4.1.2.15. N-(4-chloro-3-(trifluoromethyl)phenyl)-4-fluoro-3-nitrobenzamide (**12o**).* White solid (1.19 g, 81.2%) was obtained from **10c** and **11j**. Mp: 181–182 °C. ESI-MS m/z: 345.0 $[M+H]^+$. ^{1}H NMR (300 MHz, DMSO-d_6): δ 7.68–7.75 (2H, m, H–Ar), 7.92 (1H, d, H–Ar, J = 2.1 Hz), 8.08 (1H, d, H–Ar, J = 8.1 Hz), 8.51–8.56 (2H, m, H–Ar), 10.82 (1H, s, NHCO).

*4.1.2.16. N-(3-nitrophenyl)-4-chloro-3-(trifluoromethyl)benzamide (**15a**).* White solid (1.14 g, 82.6%) was obtained from **14a** and **7a**. Mp: 205–206 °C. ESI-MS m/z: 345.0 $[M+H]^+$. ^{1}H NMR (300 MHz, DMSO-d_6): δ 7.70 (1H, t, H–Ar, J = 8.1 Hz), 7.96–8.03 (2H, m, H–Ar), 8.20 (1H, d, H–Ar, J = 8.1 Hz), 8.30 (1H, dd, H–Ar, J = 2.1 Hz, J = 8.4 Hz), 8.45 (1H, d, H–Ar, J = 1.8 Hz), 8.78 (1H, t, H–Ar, J = 2.1 Hz), 10.96 (1H, s, NHCO).

*4.1.2.17. N-(4-methyl-3-nitrophenyl)-4-chloro-3-(trifluoromethyl) benzamide (**15b**).* White solid (1.24 g, 86.8%) was obtained from **14a** and **7b**. Mp: 189–190 °C. ESI-MS m/z: 359.0 $[M+H]^+$. ^{1}H NMR (300 MHz, DMSO-d_6): δ 2.45 (3H, s, $ArCH_3$), 7.55 (1H, d, H–Ar, J = 8.7 Hz), 7.97–8.03 (2H, m, H–Ar), 8.30 (1H, dd, H–Ar, J = 2.1 Hz, J = 8.4 Hz), 8.44 (1H, d, H–Ar, J = 1.8 Hz), 8.54 (1H, d, H–Ar, J = 2.1 Hz), 10.86 (1H, s, NHCO).

*4.1.2.18. N-(4-methyl-3-nitrophenyl)-3-(trifluoromethyl)benzamide (**15c**).* White solid (1.07 g, 82.6%) was obtained from **14b** and **7b**. Mp: 165–167 °C. ESI-MS m/z: 324.0 $[M+H]^+$. ^{1}H NMR (300 MHz, DMSO-d_6): δ 2.45 (3H, s, $ArCH_3$), 7.51 (1H, d, H–Ar, J = 7.8 Hz), 7.76 (1H, t, H–Ar, J = 7.9 Hz), 8.01 (1H, d, H–Ar, J = 8.5 Hz), 8.05 (1H, d, H–Ar, J = 8.4 Hz), 8.21 (1H, s, H–Ar), 8.29 (1H, dd, H–Ar, J = 2.1 Hz, J = 8.4 Hz), 8.67 (1H, d, H–Ar, J = 2.1 Hz), 10.80 (1H, s, NHCO).

*4.1.2.19. N-(4-methyl-3-nitrophenyl)-3-cyanobenzamide (**15d**).* White solid (0.934 g, 84.1%) was obtained from **14c** and **7b**. Mp: 162–163 °C. ESI-MS m/z: 282.1 $[M+H]^+$. ^{1}H NMR (300 MHz, DMSO-d_6): δ 2.45 (3H, s, $ArCH_3$), 7.57 (1H, dd, H–Ar, J = 1.8 Hz, J = 7.8 Hz), 7.81–7.84 (3H, m, H–Ar), 8.19 (1H, dd, H–Ar, J = 4.8 Hz, J = 9.0 Hz), 8.36 (1H, dd, H–Ar, J = 4.5 Hz, J = 8.4 Hz), 8.48 (1H, s, H–Ar), 10.79 (1H, s, NHCO).

*4.1.2.20. N-(4-methyl-3-nitrophenyl)-4-chloro-3-methylbenzamide (**15e**).* White solid (0.881 g, 72.2%) was obtained from **14d** and **7b**. Mp: 216–217 °C. ESI-MS m/z: 305.1 $[M+H]^+$. ^{1}H NMR (300 MHz, DMSO-d_6): 2.45 (3H, s, $ArCH_3$), 2.58 (3H, s, $ArCH_3$), 7.57 (2H, dd, H–Ar, J = 1.8 Hz, J = 7.8 Hz), 7.69 (1H, d, H–Ar, J = 2.1 Hz), 7.78–7.82 (3H, m, H–Ar), 10.79 (1H, s, NHCO).

*4.1.2.21. N-(4-methyl-3-nitrophenyl)-3-chlorobenzamide (**15f**).* White solid (0.950 g, 81.6%) was obtained from **14e** and **7b**. Mp: 121–123 °C. ESI-MS m/z: 291.0 $[M+H]^+$. ^{1}H NMR (300 MHz, DMSO-d_6): δ 2.47 (3H, s, $ArCH_3$), 7.50 (1H, d, H–Ar, J = 9.0 Hz), 7.69–7.77 (2H, m, H–Ar), 7.96 (1H, d, H–Ar, J = 7.8 Hz), 8.02 (1H, dd, H–Ar, J = 2.1 Hz, J = 8.4 Hz), 8.06 (1H, s, H–Ar), 8.56 (1H, d, H–Ar, J = 2.1 Hz), 10.67 (1H, s, NHCO).

*4.1.2.22. N-(4-methyl-3-nitrophenyl)-3-methoxybenzamide (**15g**).* White solid (0.948 g, 82.6%) was obtained from **14f** and **7b**. Mp: 180–182 °C. ESI-MS m/z: 287.1 $[M+H]^+$. ^{1}H NMR (300 MHz, DMSO-d_6): δ 2.47 (3H, s, $ArCH_3$), 3.84 (1H, s, OCH_3), 7.19 (1H, dd, H–Ar, J = 1.5 Hz, J = 6.3 Hz), 7.55–7.61 (3H, m, H–Ar), 8.00 (1H, dd, H–Ar, J = 2.3 Hz, J = 8.4 Hz), 8.18 (1H, d, H–Ar, J = 2.1 Hz), 8.55 (1H, d, H–Ar, J = 2.1 Hz), 10.56 (1H, s, NHCO).

*4.1.2.23. N-(4-methyl-3-nitrophenyl)-3-(dimethylamino)benzamide (**15h**).* White solid (0.968 g, 80.7%) was obtained from **14g** and **7b**. Mp: 107–109 °C. ESI-MS m/z: 300.1 $[M+H]^+$. ^{1}H NMR (300 MHz, DMSO-d_6): 2.47 (3H, s, $ArCH_3$), 3.12 (6H, s, $N(CH_3)_2$), 7.19–7.22 (2H, m, H–Ar), 7.37–7.45 (2H, m, H–Ar), 7.58 (1H, dd, H–Ar, J = 2.1 Hz, J = 8.1 Hz), 7.82–7.84 (2H, m, H–Ar), 10.66 (1H, s, NHCO).

*4.1.3. General procedure for the preparation of 3-aminobisaryl ureas and amides (**9a**–**b**, **13a**–**o** and **16a**–**h**)*

To a solution of 3-nitrobisarylurea/3-nitrobenzamide **8a**–**b**, **12a**–**o** and **15a**–**h** (3 mmol) dissolved in methanol/tetrahydrofuran (1:1, 30 mL) was added 5% palladium/carbon (3 mmol), then the reaction mixture was stirred at room temperature under hydrogen atmosphere for 3–6 h. The insoluble material was filtered off through a short bed of celite, and the filtrate was concentrated in vacuum. The crude product was purified by column chromatography over silica gel using acetic ether and petroleum ether (4:1) as eluent to give compounds **9a**–**b**, **13a**–**o** and **16a**–**h** as white or light yellow solid.

*4.1.3.1. 1-(3-Aminophenyl)-3-(4-chloro-3-(trifluoromethyl)phenyl) urea (**9a**).* Light yellow solid (0.629 g, 63.6%) was obtained from **8a**. Mp: 210–212 °C. ESI-MS m/z: 330.0 $[M+H]^+$. ^{1}H NMR (300 MHz, $CDCl_3$): δ 5.11 (2H, s, $ArNH_2$), 6.21 (1H, dd, H–Ar, J = 1.2 Hz, J = 8.1 Hz), 6.53 (1H, d, H–Ar, J = 9.0 Hz), 6.81 (1H, t, H–Ar, J = 2.1 Hz), 6.90 (1H, t, H–Ar, J = 7.8 Hz), 7.55–7.62 (2H, m, H–Ar), 8.14 (1H, d, H–Ar, J = 2.1 Hz), 8.53 (1H, s, *NH*CONH), 9.02 (1H, s, NHCO*NH*).

*4.1.3.2. 1-(3-Amino-4-methylphenyl)-3-(4-chloro-3-(trifluoromethyl)phenyl)urea (**9b**).* White solid (0.720 g, 69.8%) was obtained from **8b**. Mp: 199–201 °C. ESI-MS m/z: 344.0 $[M+H]^+$. ^{1}H NMR (300 MHz, DMSO-d_6): δ 1.98 (3H, s, $ArCH_3$), 4.76 (2H, s, $ArNH_2$), 6.55 (1H, d, H–Ar, J = 8.1 Hz), 6.78 (1H, d, H–Ar, J = 8.4 Hz), 6.87 (1H, d, H–Ar, J = 2.1 Hz), 7.54–7.63 (2H, m, H–Ar), 8.18 (1H, d, H–Ar, J = 2.1 Hz), 9.18 (1H, s, *NH*CONH), 9.82 (1H, s, NHCO*NH*).

*4.1.3.3. N-(4-chloro-3-(trifluoromethyl)phenyl)-3-aminobenzamide (**13a**).* White solid (0.665 g, 70.4%) was obtained from **12a**. Mp: 168–170 °C. ESI-MS m/z: 315.0 $[M+H]^+$. ^{1}H NMR (300 MHz, $CDCl_3$): δ 4.27 (2H, s, $ArNH_2$), 6.88–6.93 (2H, m, H–Ar), 7.09 (1H, s, H–Ar), 7.39 (2H, d, H–Ar, J = 2.1 Hz), 7.75 (1H, d, H–Ar, J = 2.1 Hz), 7.90 (1H, s, H–Ar), 8.15 (1H, s, CONH).

*4.1.3.4. N-(4-chloro-3-(trifluoromethyl)phenyl)-4-methyl-3-aminobenzamide (**13b**).* White-off solid (0.654 g, 66.3%) was obtained from **12b**. Mp: 154–156 °C. ESI-MS m/z: 329.0 $[M+H]^+$. ^{1}H NMR (300 MHz, $CDCl_3$): δ 2.24 (3H, s, $ArCH_3$), 3.80 (2H, s, $ArNH_2$), 7.13–7.18 (2H, m, H–Ar), 7.21 (1H, s, H–Ar), 7.48 (1H, d, H–Ar,

J = 8.7 Hz), 7.88 (1H, d, H–Ar, J = 8.7 Hz), 7.94 (1H, s, H–Ar), 7.95 (1H, s, CONH).

*4.1.3.5. N-(3-(trifluoromethyl)phenyl)-4-methyl-3-aminobenzamide (**13c**).* White-off solid (0.599 g, 67.2%) was obtained from **12c**. Mp: 120–121 °C. ESI-MS m/z: 294.1 $[M+H]^+$. ^{1}H NMR (300 MHz, DMSO-d_6): δ 2.12 (3H, s, $ArCH_3$), 5.09 (2H, s, $ArNH_2$), 7.05–7.12 (2H, m, H–Ar), 7.18 (1H, s, H–Ar), 7.41 (1H, d, H–Ar, J = 7.8 Hz), 7.57 (1H, t, H–Ar, J = 7.8 Hz), 8.04 (1H, d, H–Ar, J = 8.7 Hz), 8.24 (1H, s, H–Ar), 10.30 (1H, s, CONH).

*4.1.3.6. N-(3-isopropylphenyl)-4-methyl-3-aminobenzamide (**13d**).* White-off solid (0.534 g, 66.2%) was obtained from **12d**. Mp: 152–154 °C. ESI-MS m/z: 269.1 $[M+H]^+$. ^{1}H NMR (300 MHz, $CDCl_3$): δ 1.26 (6H, d, $(CH_3)_2CH$, J = 6.9 Hz), 2.20 (3H, s, $ArCH_3$), 2.90–2.93 (1H, m, $(CH_3)_2CH$), 3.77 (2H, s, $ArNH_2$), 7.00 (1H, d, H–Ar, J = 7.8 Hz), 7.09–7.15 (2H, m, H–Ar), 7.22–7.29 (2H, m, H–Ar), 7.46 (1H, d, H–Ar, J = 8.1 Hz), 7.50 (1H, s, H–Ar), 7.82 (1H, s, CONH).

*4.1.3.7. N-(3-cyanophenyl)-4-methyl-3-aminobenzamide (**13e**).* White-off solid (0.572 g, 75.7%) was obtained from **12e**. Mp: 180–182 °C. ESI-MS m/z: 252.1 $[M+H]^+$. ^{1}H NMR (300 MHz, DMSO-d_6): δ 2.12 (3H, s, $ArCH_3$), 5.10 (2H, s, $ArNH_2$), 7.08–7.11 (2H, m, H–Ar), 7.17 (1H, s, H–Ar), 7.51–7.58 (2H, m, H–Ar), 8.02–8.06 (1H, m, H–Ar), 8.24 (1H, s, H–Ar), 10.31 (1H, s, CONH).

*4.1.3.8. N-(3-fluorophenyl)-4-methyl-3-aminobenzamide (**13f**).* White-off solid (0.525 g, 71.4%) was obtained from **12f**. Mp: 142–144 °C. ESI-MS m/z: 245.1 $[M+H]^+$. ^{1}H NMR (300 MHz, DMSO-d_6): δ 2.42 (3H, s, $ArCH_3$), 5.08 (2H, s, $ArNH_2$), 6.85–6.92 (1H, m, H–Ar), 7.06 (1H, d, H–Ar, J = 8.7 Hz), 7.17 (2H, d, H–Ar, J = 4.8 Hz), 7.35 (1H, dd, H–Ar, J = 4.8 Hz, J = 8.7 Hz), 7.56 (1H, d, H–Ar, J = 8.7 Hz), 7.74 (1H, t, H–Ar, J = 4.8 Hz), 10.18 (1H, s, CONH).

*4.1.3.9. N-(4-chloro-3-methylphenyl)-4-methyl-3-aminobenzamide (**13g**).* White-off solid (0.572 g, 69.3%) was obtained from **12g**. Mp: 156–157 °C. ESI-MS m/z: 275.0 $[M+H]^+$. ^{1}H NMR (300 MHz, $CDCl_3$): δ 2.25 (3H, s, $ArCH_3$), 2.39 (3H, s, $ArCH_3$), 5.11 (2H, s, $ArNH_2$), 7.14 (2H, s, H–Ar), 7.31 (2H, d, H–Ar), 7.41 (1H, dd, H–Ar, J = 2.1 Hz, J = 8.9 Hz), 7.57 (1H, d, H–Ar, J = 2.1 Hz), 7.80 (1H, s, CONH).

*4.1.3.10. N-(3-chlorophenyl)-4-methyl-3-aminobenzamide (**13h**).* White-off solid (0.579 g, 74.0%) was obtained from **12h**. Mp: 136–138 °C. ESI-MS m/z: 261.0 $[M+H]^+$. ^{1}H NMR (300 MHz, DMSO-d_6): δ 2.12 (3H, s, $ArCH_3$), 5.08 (2H, s, $ArNH_2$), 7.06–7.16 (4H, m, H–Ar), 7.35 (1H, t, H–Ar, J = 8.1 Hz), 7.69 (1H, d, H–Ar, J = 8.1 Hz), 7.96 (1H, s, H–Ar), 10.15 (1H, s, CONH).

*4.1.3.11. N-(3-bromo-4-chlorophenyl)-4-methyl-3-aminobenzamide (**13i**).* White-off solid (0.767 g, 75.4%) was obtained from **12i**. Mp: 188–190 °C. ESI-MS m/z: 339.0 $[M+H]^+$. ^{1}H NMR (300 MHz, DMSO-d_6): δ 2.12 (3H, s, $ArCH_3$), 5.10 (2H, s, $ArNH_2$), 7.06 (2H, s, H–Ar), 7.15 (1H, s, H–Ar), 7.58 (1H, d, H–Ar, J = 8.7 Hz), 7.79 (1H, dd, H–Ar, J = 8.7 Hz), 8.28 (1H, s, H–Ar), 10.23 (1H, s, CONH).

*4.1.3.12. N-(4-trifluoromethylphenyl)-4-methyl-3-aminobenzamide (**13j**).* White-off solid (0.657 g, 74.2%) was obtained from **12j**. Mp: 125–127 °C. ESI-MS m/z: 295.0 $[M+H]^+$. ^{1}H NMR (300 MHz, DMSO-d_6): δ 2.12 (3H, s, $ArCH_3$), 5.10 (2H, s, $ArNH_2$), 7.05–7.15 (2H, m, H–Ar), 7.18 (1H, s, H–Ar), 7.69 (2H, d, H–Ar, J = 8.7 Hz), 8.00 (2H, d, H–Ar, J = 8.7 Hz), 10.34 (1H, s, CONH).

*4.1.3.13. N-(4-chloro-3-trifluoromethylphenyl)-4-chloro-3-aminobenzamide (**13k**).* White-off solid (0.752 g, 71.8%) was obtained from **12k**. Mp: 136–138 °C. ESI-MS m/z: 349.0 $[M+H]^+$. ^{1}H NMR (300 MHz, DMSO-d_6): δ 5.64 (2H, s, $ArNH_2$), 7.12 (1H, d, H–Ar, J = 8.1 Hz), 7.34–7.37 (2H, m, H–Ar), 7.70 (1H, t, H–Ar, J = 8.7 Hz), 8.09 (1H, d, H–Ar, J = 8.7 Hz), 8.33 (1H, s, H–Ar), 10.54 (1H, s, CONH).

*4.1.3.14. N-(3-trifluoromethylphenyl)-4-chloro-3-aminobenzamide (**13l**).* White-off solid (0.765 g, 81.0%) was obtained from **12l**. Mp: 124–126 °C. ESI-MS m/z: 315.0 $[M+H]^+$. ^{1}H NMR (300 MHz, DMSO-d_6): δ 5.63 (2H, s, $ArNH_2$), 7.13 (1H, dd, H–Ar, J = 2.4 Hz, J = 8.4 Hz), 7.35 (1H, d, H–Ar, J = 2.4 Hz), 7.37 (1H, s, H–Ar), 7.44 (1H, d, H–Ar, J = 7.8 Hz), 7.59 (1H, t, H–Ar, J = 8.4 Hz), 8.03 (1H, d, H–Ar, J = 8.4 Hz), 8.22 (1H, s, H–Ar), 10.44 (1H, s, CONH).

*4.1.3.15. N-(3-isopropylphenyl)-4-chloro-3-aminobenzamide (**13m**).* White-off solid (0.587 g, 67.7%) was obtained from **12m**. Mp: 147–148 °C. ESI-MS m/z: 289.1 $[M+H]^+$. ^{1}H NMR (300 MHz, DMSO-d_6): δ 1.22 (6H, d, $CH(CH_3)_2$, J = 6.9 Hz), 2.84–2.93 (1H, m, $CH(CH_3)_2$), 5.15 (2H, s, $ArNH_2$), 6.97 (1H, d, H–Ar, J = 7.8 Hz), 7.28 (1H, d, H–Ar, J = 7.8 Hz), 7.54–7.59 (2H, m, H–Ar), 7.97 (1H, t, H–Ar, J = 8.4 Hz), 8.26 (1H, dd, H–Ar, J = 2.1 Hz, J = 8.4 Hz), 8.63 (1H, d, H–Ar, J = 2.1 Hz), 10.43 (1H, s, CONH).

*4.1.3.16. N-(3,4-dichlorophenyl)-4-chloro-3-aminobenzamide (**13n**).* White-off solid (0.691 g, 73.2%) was obtained from **12n**. Mp: 182–184 °C. ESI-MS m/z: 315.0 $[M+H]^+$. ^{1}H NMR (300 MHz, DMSO-d_6): δ 5.65 (2H, s, $ArNH_2$), 7.10 (1H, dd, H–Ar, J = 2.1 Hz, J = 8.1 Hz), 7.32–7.37 (2H, m, H–Ar), 7.61 (1H, d, H–Ar, J = 8.7 Hz), 7.73 (1H, dd, H–Ar, J = 2.4 Hz, J = 8.7 Hz), 8.13 (1H, d, H–Ar, J = 2.4 Hz), 10.42 (1H, s, CONH).

*4.1.3.17. N-(4-chloro-3-(trifluoromethyl)phenyl)-4-fluoro-3-aminobenzamide (**13o**).* White-off solid (0.722 g, 72.3%) was obtained from **12o**. Mp: 174–175 °C. ESI-MS m/z: 333.0 $[M+H]^+$. ^{1}H NMR (300 MHz, DMSO-d_6): δ 5.43 (2H, s, $ArNH_2$), 7.15 (2H, d, H–Ar, J = 8.7 Hz), 7.35 (1H, d, H–Ar, J = 9.0 Hz), 7.70 (1H, d, H–Ar, J = 9.0 Hz), 8.09 (1H, dd, H–Ar, J = 2.4 Hz, J = 8.7 Hz), 8.34 (1H, d, H–Ar, J = 2.4 Hz), 10.49 (1H, s, CONH).

*4.1.3.18. N-(3-aminophenyl)-4-chloro-3-(trifluoromethyl)benzamide (**16a**).* White-off solid (0.801 g, 84.8%) was obtained from **15a**. Mp: 194–195 °C. ESI-MS m/z: 315.0 $[M+H]^+$. ^{1}H NMR (300 MHz, DMSO-d_6): δ 5.67 (2H, s, $ArNH_2$), 7.03 (1H, dd, H–Ar, J = 4.8 Hz, J = 7.8 Hz), 7.32 (1H, t, H–Ar, J = 7.8 Hz), 7.46 (1H, d, H–Ar, J = 7.8 Hz), 7.56 (1H, d, H–Ar, J = 7.8 Hz), 7.92 (1H, d, H–Ar, J = 8.4 Hz), 8.28 (1H, d, H–Ar, J = 2.1 Hz, J = 8.4 Hz), 8.37 (1H, dd, H–Ar, J = 2.1 Hz, J = 4.8 Hz), 10.51 (1H, s, CONH).

*4.1.3.19. N-(3-amino-4-methylphenyl)-4-chloro-3-(trifluoromethyl) benzamide (**16b**).* White-off solid (0.836 g, 84.7%) was obtained from **15a**. Mp: 180–182 °C. ESI-MS m/z: 329.0 $[M+H]^+$. ^{1}H NMR (300 MHz, DMSO-d_6): δ 2.03 (3H, s, $ArCH_3$), 4.91 (2H, s, $ArNH_2$), 6.82 (1H, d, H–Ar, J = 8.1 Hz), 6.88 (1H, d, H–Ar, J = 8.1 Hz), 7.08 (1H, s, H–Ar), 7.89 (1H, d, H–Ar, J = 8.7 Hz), 8.23 (1H, d, H–Ar, J = 8.7 Hz), 8.34 (1H, s, H–Ar), 10.18 (1H, s, CONH).

*4.1.3.20. N-(3-amino-4-methylphenyl)-3-(trifluoromethyl)benzamide (**16c**).* White-off solid (0.736 g, 83.4%) was obtained from **15c**. Mp: 157–159 °C. ESI-MS m/z: 294.1 $[M+H]^+$. ^{1}H NMR (300 MHz, DMSO-d_6): δ 2.03 (3H, s, $ArCH_3$), 4.87 (2H, s, $ArNH_2$), 6.80–6.89 (2H, m, H–Ar), 7.11 (1H, d, H–Ar, J = 2.1 Hz), 7.76 (1H, t, H–Ar, J = 7.8 Hz), 7.94 (1H, d, H–Ar, J = 7.8 Hz), 8.21–8.25 (2H, m, H–Ar), 10.13 (1H, s, CONH).

*4.1.3.21. N-(3-amino-4-methylphenyl)-3-cyanobenzamide (**16d**).* White-off solid (0.624 g, 82.5%) was obtained from **15d**. Mp:

166–167 °C. ESI-MS *m/z*: 252.1 $[M+H]^+$. ^{1}H NMR (300 MHz, DMSO-d_6): δ 2.44 (3H, s, $ArCH_3$), 5.42 (2H, s, $ArNH_2$), 6.98 (1H, dd, H–Ar, *J* = 4.8 Hz, *J* = 7.8 Hz), 7.25 (1H, d, H–Ar, *J* = 8.4 Hz), 7.38 (1H, dd, H–Ar, *J* = 2.1 Hz, *J* = 8.1 Hz), 7.74 (1H, t, H–Ar, *J* = 7.8 Hz), 8.04–8.07 (1H, m, H–Ar), 8.27 (1H, d, H–Ar, *J* = 8.1 Hz), 8.36 (1H, dd, H–Ar, *J* = 2.1 Hz, *J* = 4.8 Hz), 10.33 (1H, s, CONH).

*4.1.3.22. N-(3-amino-4-methylphenyl)-4-chloro-3-methylbenzamide (**16e**).* White-off solid (0.668 g, 81.0%) was obtained from **15e**. Mp: 176–178 °C. ESI-MS *m/z*: 275.1 $[M+H]^+$. ^{1}H NMR (300 MHz, DMSO-d_6): δ 2.21 (3H, s, $ArCH_3$), 2.34 (3H, s, $ArCH_3$), 5.87 (2H, s, $ArNH_2$), 6.83 (1H, s, H–Ar), 6.92–6.96 (2H, m, H–Ar), 7.57 (1H, d, H–Ar, *J* = 7.8 Hz), 7.95 (1H, d, H–Ar, *J* = 7.8 Hz), 8.17 (1H, dd, H–Ar, *J* = 2.1 Hz, *J* = 4.8 Hz), 10.15 (1H, s, CONH).

*4.1.3.23. N-(3-amino-4-methylphenyl)-3-chlorobenzamide (**16f**).* White-off solid (0.621 g, 79.3%) was obtained from **15f**. Mp: 132–134 °C. ESI-MS *m/z*: 261.0 $[M+H]^+$. ^{1}H NMR (300 MHz, $CDCl_3$): δ 2.46 (3H, s, $ArCH_3$), 5.21 (2H, s, $ArNH_2$), 7.02–7.06 (1H, m, H–Ar), 7.24 (1H, d, H–Ar, *J* = 8.7 Hz), 7.47 (1H, d, H–Ar, *J* = 8.1 Hz), 7.57 (1H, t, H–Ar, *J* = 7.8 Hz), 7.66 (1H, d, H–Ar, *J* = 8.7 Hz), 7.94 (1H, d, H–Ar, *J* = 7.8 Hz), 8.36 (1H, dd, H–Ar, *J* = 2.1 Hz, *J* = 4.8 Hz), 10.30 (1H, s, CONH).

*4.1.3.24. N-(3-amino-4-methylphenyl)-3-methoxybenzamide (**16g**).* White-off solid (0.617 g, 80.1%) was obtained from **15g**. Mp: 116–117 °C. ESI-MS *m/z*: 257.1 $[M+H]^+$. ^{1}H NMR (300 MHz, $CDCl_3$): δ 2.15 (3H, s, $ArCH_3$), 3.65 (2H, s, $ArNH_2$), 3.87 (3H, s, OCH_3), 6.72 (1H, dd, H–Ar, *J* = 2.1 Hz, *J* = 7.8 Hz), 7.01 (1H, d, H–Ar, *J* = 8.1 Hz), 7.04–7.09 (1H, m, H–Ar), 7.29 (1H, d, H–Ar, *J* = 2.1 Hz), 7.38 (2H, d, H–Ar, *J* = 8.1 Hz), 7.41–7.43 (1H, m, H–Ar), 7.67 (1H, s, CONH).

*4.1.3.25. N-(3-amino-4-methylphenyl)-3-(dimethylamino)benzamide (**16h**).* White-off solid (0.658 g, 81.3%) was obtained from **15h**. Mp: 170–172 °C. ESI-MS *m/z*: 270.1 $[M+H]^+$. ^{1}H NMR (300 MHz, $CDCl_3$): δ 2.42 (3H, s, $ArCH_3$), 2.97 (6H, s, $N(CH_3)_2$), 4.74 (2H, s, $ArNH_2$), 6.92 (1H, dd, H–Ar, *J* = 1.6 Hz, *J* = 8.1 Hz), 7.02 (1H, dd, H–Ar, *J* = 4.8 Hz, *J* = 7.8 Hz), 7.23–7.25 (2H, m, H–Ar), 7.31 (1H, t, H–Ar, *J* = 8.1 Hz), 7.43 (1H, dd, H–Ar, *J* = 2.1 Hz, *J* = 8.1 Hz), 8.34 (1H, dd, H–Ar, *J* = 1.8 Hz, *J* = 4.8 Hz), 10.10 (1H, s, CONH).

*4.1.4. 6-Chloro-9-(tetrahydro-2H-pyran-2-yl)-9H-purine (**18**)*

A mixture of 6-chloro-9*H*-purine **17** (2.01 g, 13 mmol), 3,4-dihydro-2*H*-pyran (3.30 g, 39 mmol) and TsOH (516 mg, 0.3 mmol) dissolved in anhydrous ethyl acetate (30 mL) was refluxed for 3 h. Then cooled to the room temperature and washed with water and brine. The organic layer was dried (anhydrous Na_2SO_4) and concentrated to afford the compound **18** (2.62 g, 83.2%) as a yellow oil. ESI-MS *m/z*: 239.0 $[M+H]^+$. ^{1}H NMR (300 MHz, DMSO-d_6): δ 1.58–1.64 (2H, m, H-pyran), 1.69–1.78 (1H, m, H-pyran), 1.97–2.05 (2H, m, H-pyran), 2.32–2.37 (1H, m, H-pyran), 3.69–3.77 (1H, m, H-pyran), 4.03 (1H, d, *J* = 5.4 Hz, H-pyran), 5.80 (1H, dd, *J* = 2.1 Hz, *J* = 10.9 Hz, H-pyran), 8.81 (1H, s, H-purine), 8.91 (1H, s, H-purine).

*4.1.5. 6-(2-Fluoropyridin-3-yl)-9-(tetrahydro-2H-pyran-2-yl)-9H-purine (**19**)*

A mixture of compound **18** (2.38 g, 10 mmol), (2-fluoropyridin-3-yl)boronic acid (2.10 g, 15 mmol), $PdCl_2$(dppf) (150 mg, 0.2 mmol) and Na_2CO_3 (4.23 g, 40 mmol) dissolved in 1,4-dioxane/H_2O (1:7) (40 mL) was refluxed under nitrogen for 14 h. After cooling to room temperature, the mixture was diluted in 50 mL H_2O. The aqueous layer was extracted with EtOAc (3 × 50 mL). The combined organic layers were washed with saturated solution of NaCl and then dried over anhydrous $MgSO_4$, filtered and evaporated. The resulting solid was obtained by a column chromatography, using a mixture of acetic ether and petroleum ether (1:1) purified as eluent (1.54 g, 51.5%). Mp: 132–133 °C. ESI-MS *m/z*: 300.2 $[M+H]^+$. ^{1}H NMR (300 MHz, DMSO-d_6): δ 1.60–1.67 (2H, m, H-pyran), 1.75–1.82 (1H, m, H-pyran), 1.99–2.08 (2H, m, H-pyran), 2.34–2.41 (1H, m, H-pyran), 3.71–3.80 (1H, m, H-pyran), 4.05 (1H, d, *J* = 11.1 Hz, H-pyran), 5.86 (1H, dd, *J* = 2.1 Hz, *J* = 10.8 Hz, H-pyran), 7.59–7.64 (1H, m, H-pyridine), 8.47 (1H, dd, H-pyridine, *J* = 1.0 Hz, *J* = 3.0 Hz), 8.54–8.60 (1H, m, H-pyridine), 8.90 (1H, s, H-purine), 9.09 (1H, s, H-purine).

*4.1.6. General procedure for the preparation of target compounds (**6a**–**b**, **20a**–**o** and **21a**–**h**)*

A mixture of **9a**–**b**, **13a**–**o** or **16a**–**h** (0.55 mmol) and the intermediate **20** (165 mg, 0.5 mmol) in anhydrous tetrahydrofuran (30 mL) was stirred under nitrogen at 0 °C for 10 min. Then LiHMDS (Lithium hexamethyldisilazide, 1 mol/L THF, 0.5 mL) was added dropwise to the reaction mixture at 0 °C. Reaction mixture was further stirred for 2–6 h at room temperature. The mixture was quenched with H_2O (40 mL) and EtOAc (40 mL). The aqueous phase was washed with EtOAc (3 × 40 mL) and dried over anhydrous Na_2SO_4. After filtration, the solvent was removed under reduced pressure. Afterward, the residue was dissolved in MeOH (30 mL) and stirred at room temperature. Then 2 mL diluted hydrochloric acid (1 M) was added dropwise to the reaction mixture. After stirring for 3 h at room temperature, adjust the pH to 8-9 by 10% sodium carbonate solution. The solvent was evaporated under reduced pressure. The crude compound was purified by column chromatography over silica gel by using petroleum/ether acetate (1:1–1:2) as eluent to give compounds **6a**–**b**, **20a**–**o** and **21a**–**h** as yellow solid.

*4.1.6.1. 1-(3-((3-(9H-purin-6-yl)pyridin-2-yl)amino)phenyl)-3-(4-chloro-3-(trifluoromethyl)phenyl)urea (**6a**).* Yellow solid (91 mg, 34.7%) was obtained from **9a**. Mp: 270–272 °C. HRMS (ESI$^+$) *m/z* calculated for $C_{24}H_{16}ClF_3N_8O$ $[M+H]^+$ 525.1160; found, 525.1164. ^{1}H NMR (300 MHz, DMSO-d_6): δ 7.00 (1H, dd, *J* = 4.8 Hz, *J* = 7.8 Hz), 7.21–7.26 (2H, m), 7.36 (1H, d, *J* = 6.6 Hz), 7.56–7.66 (2H, m, H–Ar), 8.01 (1H, s, H–Ar), 8.10 (1H, d, *J* = 1.8 Hz), 8.34 (1H, dd, *J* = 1.8 Hz, *J* = 4.8 Hz), 8.68 (1H, s), 8.86 (1H, s, H-purine), 9.07 (1H, s, H-purine), 9.14 (1H, s, *NH*CONH), 9.88 (1H, s, NHCO*NH*), 12.52 (1H, s), 13.81 (1H, s, 9*H*-purine). ^{13}C NMR (75 MHz, DMSO-d_6): δ 110.20, 112.28, 112.88, 113.85, 114.42, 116.57, 120.97, 122.17, 122.87, 124.58, 126.62 (q, CF_3), 128.86, 129.33, 131.86, 139.35, 139.49, 140.87, 141.67, 144.62, 149.74, 150.04, 152.33, 153.03, 153.93 (NHCONH).

*4.1.6.2. 1-(3-((3-(9H-purin-6-yl)pyridin-2-yl)amino)-4-methylphenyl)-3-(4-chloro-3-(trifluoromethyl)phenyl)urea (**6b**).* Yellow solid (88 mg, 32.7%) was obtained from **9b**. Mp: 246–248 °C. HRMS (ESI$^+$) *m/z* calculated for $C_{25}H_{18}ClF_3N_8O$ $[M+H]^+$ 539.1317; found, 539.1316. ^{1}H NMR (300 MHz, DMSO-d_6): δ 2.42 (3H, s, $ArCH_3$), 7.05 (1H, dd, *J* = 4.8 Hz, *J* = 7.8 Hz), 7.17 (1H, d, *J* = 8.4 Hz), 7.28 (1H, dd, *J* = 2.1 Hz, *J* = 8.1 Hz), 7.61 (2H, t, *J* = 4.8 Hz), 8.10 (1H, s), 8.35 (1H, dd, *J* = 1.8 Hz, *J* = 4.8 Hz), 8.39 (1H, d, *J* = 1.8 Hz), 8.64 (1H, s), 8.73 (1H, s, H-purine), 8.97 (1H, s, H-purine), 9.06 (1H, s, NHCO*NH*), 9.75 (1H, s, *NH*CONH), 12.33 (1H, s), 13.78 (1H, s, 9*H*-purine). ^{13}C NMR (75 MHz, DMSO-d_6): δ 19.17 (CH_3), 111.24, 112.42, 113.11, 113.62, 116.45, 120.96, 121.58, 121.98, 122.67, 124.58, 126.63 (q, CF_3), 129.33, 130.06, 131.78, 137.11, 139.21, 139.44, 141.71, 144.46, 149.63, 149.74, 152.38, 153.01, 154.11 (NHCONH).

*4.1.6.3. 3-((3-(9H-purin-6-yl)pyridin-2-yl)amino)-N-(4-chloro-3-(trifluoromethyl)phenyl)benzamide (**20a**).* Yellow solid (74 mg, 29.1%) was obtained from **13a**. Mp: 334–335 °C. HRMS (ESI$^+$) *m/z* calculated for $C_{24}H_{15}ClF_3N_7O$ $[M+H]^+$ 510.1051; found, 510.1048. ^{1}H

NMR (300 MHz, DMSO-d_6): δ 7.06 (1H, dd, J = 4.8 Hz, J = 7.8 Hz), 7.51 (1H, t, J = 8.1 Hz), 7.59 (1H, d, J = 7.8 Hz), 7.73 (1H, d, J = 8.7 Hz), 8.14–8.18 (2H, m), 8.36–8.38 (2H, m), 8.45 (1H, d, J = 2.4 Hz), 8.56 (1H, s, H-purine), 9.10 (1H, s, H-purine), 9.81 (1H, d, J = 6.7 Hz), 10.96 (1H, s, CONH), 12.98 (1H, s). ^{13}C NMR (75 MHz, DMSO-d_6): δ 113.89, 114.28, 119.11, 120.76, 121.70, 123.13, 123.88, 124.09, 125.08, 126.38 (q, CF_3), 128.66, 130.18, 131.80, 134.73, 138.87, 140.87, 141.56, 147.55, 149.25, 149.40, 150.69, 153.80, 155.48, 166.16 (NHCO).

*4.1.6.4. 3-((3-(9H-purin-6-yl)pyridin-2-yl)amino)-N-(4-chloro-3-(trifluoromethyl)phenyl)-4-methylbenzamide (**20b**).* Yellow solid (71 mg, 27.5%) was obtained from **13b**. Mp: 315–317 °C. HRMS (ESI$^+$) m/z calculated for $C_{25}H_{17}ClF_3N_7O$ $[M+H]^+$ 524.1208; found, 524.1213. ^{1}H NMR [300 MHz, DMSO-d_6]: δ 2.54 (3H, s, $ArCH_3$), 7.07 (1H, dd, J = 4.8 Hz, J = 7.8 Hz), 7.45 (1H, d, J = 8.7 Hz), 7.59 (1H, d, J = 8.7 Hz), 7.71 (1H, d, J = 8.7 Hz), 8.13 (1H, d, J = 8.7 Hz), 8.37 (1H, d, J = 1.8 Hz), 8.38–8.40 (1H, m), 8.73 (1H, s), 8.95 (1H, s, H-purine), 9.10 (1H, s, H-purine), 9.83 (1H, s), 10.56 (1H, s, CONH), 12.45 (1H, s), 13.86 (1H, s, 9*H*-purine). ^{13}C NMR (75 MHz, DMSO-d_6): δ 18.79 (CH_3), 113.21, 114.11, 118.86 (q, CF_3), 120.44, 120.96, 121.11, 123.98, 124.57, 124.79, 126.33, 126.74, 129.32, 130.01, 131.84, 132.24, 132.38, 138.83, 139.25, 141.73, 144.71, 149.91, 149.96, 154.10, 166.16 (CONH). IR (KBr, cm^{-1}): 3186, 3092, 2989, 2837, 1674, 1593, 1541, 1381, 924, 761.

*4.1.6.5. 3-((3-(9H-purin-6-yl)pyridin-2-yl)amino)-4-methyl-N-(3-(trifluoromethyl)phenyl)benzamide (**20c**).* Yellow solid (80 mg, 33.4%) was obtained from **13c**. Mp: 288–290 °C. HRMS (ESI$^+$) m/z calculated for $C_{25}H_{18}F_3N_7O$ $[M+H]^+$ 490.1598; found, 490.1602. ^{1}H NMR [300 MHz, DMSO-d_6]: δ 2.54 (3H, s, $ArCH_3$), 7.07 (1H, dd, J = 4.8 Hz, J = 7.8 Hz), 7.44 (2H, d, J = 8.1 Hz), 7.60 (2H, t, J = 7.8 Hz), 8.07 (1H, d, J = 8.7 Hz), 8.28 (1H, s), 8.37 (1H, dd, J = 4.8 Hz, J = 7.8 Hz), 8.73 (1H, s), 8.94 (1H, s, H-purine), 9.5 (1H, s, H-purine), 9.82 (1H, s), 10.47 (1H, s, NHCO), 12.44 (1H, s), 13.85 (1H, s, 9*H*-purine). ^{13}C NMR (75 MHz, DMSO-d_6): δ 18.77 (CH_3), 113.18, 114.02, 116.27 (d, J = 4.1 Hz), 119.64 (d, J = 3.6 Hz), 120.44, 121.07, 122.34, 123.67, 125.96, 128.67, 129.08, 129.63 (q, CF_3), 129.95, 132.16, 132.52, 139.22, 140.12, 141.71, 144.69, 149.88, 149.91, 151.95, 154.11, 166.17 (CONH). IR (KBr, cm^{-1}): 3428, 3088, 2988, 2826, 1670, 1576, 1483, 799, 758, 706.

*4.1.6.6. 3-((3-(9H-purin-6-yl)pyridin-2-yl)amino)-N-(3-isopropylphenyl)-4-methylbenzamide (**20d**).* Yellow solid (65 mg, 28.1%) was obtained from **13c**. Mp: 156–158 °C. HRMS (ESI$^+$) m/z calculated for $C_{27}H_{25}N_7O$ $[M+H]^+$ 464.2193; found, 464.2192. ^{1}H NMR [300 MHz, DMSO-d_6]: δ 1.22 (6H, d, $(CH_3)_2CH$, J = 6.9 Hz), 2.53 (3H, s, $ArCH_3$), 2.87–2.89 (1H, m, $(CH_3)_2CH$), 6.97 (1H, d, J = 7.8 Hz), 7.05 (1H, dd, J = 4.8 Hz, J = 7.8 Hz), 7.25 (1H, t, J = 8.7 Hz), 7.41 (1H, d, J = 8.7 Hz), 7.57–7.64 (2H, m), 7.68 (1H, s), 8.37 (1H, dd, J = 1.8 Hz, J = 4.8 Hz), 8.72 (1H, s), 8.87 (1H, s, H-purine), 9.10 (1H, s, H-purine), 9.81 (1H, s), 10.07 (1H, s, NHCO), 12.39 (1H, s), 13.85 (1H, s, 9*H*-purine). ^{13}C NMR (75 MHz, DMSO-d_6): δ 18.70 (CH_3), 23.81 ($CH(CH_3)_2$), 33.50 ($CH(CH_3)_2$), 113.16, 113.96, 117.94, 118.31, 120.63, 121.10, 121.51, 128.35, 129.37, 129.87, 131.84, 133.22, 139.13, 139.31, 141.71, 144.63, 148.74, 149.91, 149.92, 152.04, 152.92, 154.21, 165.76 (CONH). IR (KBr, cm^{-1}): 3082, 2959, 2918, 2849, 1626, 1587, 1568, 1530, 926, 768.

*4.1.6.7. 3-((3-(9H-purin-6-yl)pyridin-2-yl)amino)-N-(3-cyanophenyl)-4-methylbenzamide (**20e**).* Yellow solid (82 mg, 41.0%) was obtained from **13e**. Mp: 328–329 °C. HRMS (ESI$^+$) m/z calculated for $C_{25}H_{18}N_8O$ $[M+H]^+$ 447.1676; found 447.1674. ^{1}H NMR [300 MHz, DMSO-d_6]: δ 2.49 (3H, s, $ArCH_3$), 7.07 (1H, dd, J = 4.8 Hz, J = 7.8 Hz), 7.44 (1H, d, J = 7.8 Hz), 7.54–7.61 (3H, m), 8.05–8.09 (1H, m), 8.28 (1H, d, J = 1.2 Hz), 8.36–8.38 (1H, m), 8.73 (1H, s), 8.94 (1H, s, H-purine), 9.10 (1H, s, H-purine), 9.84 (1H, d, J = 6.9 Hz), 10.47 (1H, s, NHCO), 12.46 (1H, s), 13.86 (1H, s, 9*H*-purine). ^{13}C NMR (75 MHz, DMSO-d_6): δ 18.77 (CH_3), 111.35, 113.18, 114.09, 118.71 (CN), 120.39, 121.10, 122.89, 124.72, 126.84, 129.33, 129.98, 132.24, 132.37, 139.20, 140.11, 141.70, 144.76, 149.93, 151.93, 152.97, 153.31, 154.07, 165.37, 166.12 (NHCO). IR (KBr, cm^{-1}): 3431, 3084, 2986, 2822, 1699, 1578, 1483, 858, 791, 762.

*4.1.6.8. 3-((3-(9H-purin-6-yl)pyridin-2-yl)amino)-N-(3-fluorophenyl)-4-methylbenzamide (**20f**).* Yellow solid (64 mg, 30.1%) was obtained from **13f**. Mp: 315–317 °C. HRMS (ESI$^+$) m/z calculated for $C_{24}H_{18}FN_7O$ $[M+H]^+$ 440.1630; found, 440.1626 ^{1}H NMR [300 MHz, DMSO-d_6]: δ 2.54 (3H, s, $ArCH_3$), 6.88–6.94 (1H, m), 7.06 (1H, dd, J = 4.8 Hz, J = 7.8 Hz), 7.34–7.44 (2H, m) 7.55–7.59 (2H, m), 7.74–7.80 (1H, m), 8.37 (1H, dd, J = 1.8 Hz, J = 4.8 Hz), 8.73 (1H, s), 8.91 (1H, s, H-purine), 9.10 (1H, s, H-purine), 9.83 (1H, s), 10.35 (1H, s, CONH), 12.43 (1H, s), 13.85 (1H, s, 9*H*-purine). ^{13}C NMR (75 MHz, DMSO-d_6): δ 18.63 (CH_3), 106.70, 107.04, 109.97, 113.20, 114.06, 115.87 (d, J = 2.6 Hz), 120.44, 121.10, 129.36, 130.01 (d, J = 4.5 Hz), 130.14, 132.75, 139.18, 141.11, 141.72, 144.82, 149.92, 151.93, 153.05, 154.12, 160.43, 163.63, 166.07 (NHCO). IR (KBr, cm^{-1}): 3433, 3098, 2990, 2847, 1674, 1599, 1570, 1530, 860, 760.

*4.1.6.9. 3-((3-(9H-purin-6-yl)pyridin-2-yl)amino)-N-(4-chloro-3-methylphenyl)-4-methylbenzamide (**20g**).* Yellow solid (83 mg, 36.6%) was obtained from **13g**. Mp: 303–305 °C. HRMS (ESI$^+$) m/z calculated for $C_{25}H_{20}ClN_7O$ $[M+H]^+$ 470.1491; found, 470.1489. ^{1}H NMR [300 MHz, DMSO-d_6]: δ 2.33 (3H, s, $ArCH_3$), 2.53 (3H, s, $ArCH_3$), 7.06 (1H, dd, J = 4.8 Hz, J = 7.8 Hz), 7.38 (1H, d, J = 8.7 Hz), 7.42 (1H, d, J = 8.7 Hz), 7.58 (1H, d, J = 7.8 Hz) 7.65 (1H, dd, J = 2.4 Hz, J = 4.8 Hz), 7.81 (1H, d, J = 2.4 Hz), 8.37 (1H, dd, J = 1.8 Hz, J = 4.8 Hz), 8.73 (1H, s), 8.90 (1H, s, H-purine), 9.10 (1H, s, H-purine), 9.82 (1H, s), 10.21 (1H, s, NHCO), 12.42 (1H, s), 13.86 (1H, s, 9*H*-purine). ^{13}C NMR (75 MHz, DMSO-d_6): δ 18.76 (CH_3), 19.82 (CH_3), 113.16, 114.02, 119.39, 120.48, 121.06, 122.65, 127.31, 128.74, 129.44, 129.91, 131.94, 132.85, 135.29, 138.21, 139.14, 141.72, 144.64, 149.90, 149.94, 151.99, 152.98, 154.13, 165.80 (NHCO). IR (KBr, cm^{-1}): 3431, 3341, 3092, 2972, 2824, 1657, 1572, 1535, 827, 764.

*4.1.6.10. 3-((3-(9H-purin-6-yl)pyridin-2-yl)amino)-N-(3-chlorophenyl)-4-methylbenzamide (**20h**).* Yellow solid (77 mg, 34.3%) was obtained from **13h**. Mp: 278–280 °C. HRMS (ESI$^+$) m/z calculated for $C_{24}H_{18}ClN_7O$ $[M+H]^+$ 456.1334; found, 456.1331. ^{1}H NMR [300 MHz, DMSO-d_6]: δ 2.53 (3H, s, $ArCH_3$), 7.07 (1H, dd, J = 4.8 Hz, J = 7.8 Hz), 7.15 (1H, d, J = 8.7 Hz), 7.35–7.44 (2H, m), 7.58 (1H, d, J = 8.7 Hz), 7.73 (1H, d, J = 8.7 Hz), 7.99 (1H, s), 8.37 (1H, d, J = 4.8 Hz), 8.73 (1H, s), 8.91 (1H, s, H-purine), 9.10 (1H, s, H-purine), 9.83 (1H, s), 10.32 (1H, s, CONH), 12.43 (1H, s), 13.85 (1H, s, 9*H*-purine). ^{13}C NMR (75 MHz, DMSO-d_6): δ 17.68 (CH_3), 111.73, 113.58, 117.48, 119.77, 120.36, 122.03, 127.94, 128.44, 129.96, 130.30, 132.06, 132.60, 134.51, 134.87, 138.94, 142.19, 144.56, 144.85, 146.47, 148.02, 152.43, 153.88, 164.78 (NHCO). IR (KBr, cm^{-1}): 3430, 3088, 2988, 2834, 1667, 1595, 1526, 858, 768.

*4.1.6.11. 3-((3-(9H-purin-6-yl)pyridin-2-yl)amino)-N-(3-bromo-4-chlorophenyl)-4-methylbenzamide (**20i**).* Yellow solid (65 mg, 30.0%) was obtained from **13i**. Mp: 335–336 °C. HRMS (ESI$^+$) m/z calculated for $C_{24}H_{17}BrClN_7O$ $[M+H]^+$ 534.0439; found, 534.0435. ^{1}H NMR [300 MHz, DMSO-d_6]: δ 2.53 (3H, s, $ArCH_3$), 7.06 (1H, dd, J = 4.8 Hz, J = 7.8 Hz), 7.43 (1H, d, J = 8.7 Hz), 7.56–7.61 (2H, m), 7.82 (1H, dd, J = 2.4 Hz, J = 8.7 Hz), 8.32 (1H, d, J = 2.4 Hz), 8.37 (1H, dd, J = 1.8 Hz, J = 4.8 Hz), 8.73 (1H, s, H-purine), 8.93 (1H, d, J = 1.8 Hz), 9.10 (1H, s, H-purine), 9.83 (1H, s), 10.40 (1H, s, CONH), 12.44 (1H, s), 13.85 (1H, s, 9*H*-purine). ^{13}C NMR (75 MHz, DMSO-d_6): δ 18.79 (CH_3), 113.19, 114.09, 120.41, 120.66, 121.03, 121.08, 124.46, 126.83,

129.43, 129.98, 130.21, 132.24, 132.40, 139.21, 139.42, 141.72, 144.71, 149.90, 149.95,151.96, 153.02, 154.10, 166.02 (NHCO). IR (KBr, cm^{-1}): 3343, 3088, 2969, 2828, 1659, 1580, 1528, 866, 800, 762.

*4.1.6.12. 3-((3-(9H-purin-6-yl)pyridin-2-yl)amino)-4-methyl-N-(4-(trifluoromethyl)phenyl)benzamide (**20j**).* Yellow solid (91 mg, 37.8%) was obtained from **13j**. Mp: 304–306 °C. HRMS (ESI^+) *m/z* calculated for $C_{25}H_{18}F_3N_7O$ $[M+H]^+$ 490.1598; found, 490.1592. ^1H NMR [300 MHz, DMSO-d_6]: δ 2.54 (3H, s, $ArCH_3$), 7.07 (1H, dd, $J = 4.8$ Hz, $J = 7.8$ Hz), 7.44 (1H, d, $J = 8.4$ Hz), 7.60 (1H, dd, $J = 1.8$ Hz, $J = 7.8$ Hz), 7.72 (2H, d, $J = 8.7$ Hz), 8.04 (2H, d, $J = 8.4$ Hz), 8.37 (1H, dd, $J = 2.1$ Hz, $J = 4.8$ Hz), 8.73 (1H, s), 8.94 (2H, d, $J = 1.5$ Hz), 9.11 (1H, s, H-purine), 10.50 (1H, s, CONH), 12.45 (1H, s), 13.86 (1H, s, 9*H*-purine). ^{13}C NMR (75 MHz, DMSO-d_6): δ 17.68 (CH_3), 107.90, 111.58, 113.56, 120.38, 124.12, 124.67 (q, CF_3), 125.27, 125.32, 127.83, 127.96, 128.44, 130.09, 133.73, 134.47, 134.85, 137.58, 142.28, 144.52, 144.83, 146.45, 148.04, 152.43, 153.89, 164.72 (NHCO). IR (KBr, cm^{-1}): 3437, 351, 2992, 2839, 1595, 1570, 1528, 845, 766.

*4.1.6.13. 3-((3-(9H-purin-6-yl)pyridin-2-yl)amino)-4-chloro-N-(4-chloro-3-(trifluoromethyl)phenyl)benzamide (**20k**).* Yellow solid (93 g, 35.6%) was obtained from **13k**. Mp: 313–315 °C. HRMS (ESI^+) *m/z* calculated for $C_{24}H_{14}Cl_2F_3N_7O$ $[M+H]^+$ 544.0662; found, 544.0666. ^1H NMR [300 MHz, DMSO-d_6]: δ 7.19 (1H, dd, $J = 4.8$ Hz, $J = 8.1$ Hz), 7.61 (1H, dd, $J = 2.1$ Hz, $J = 8.1$ Hz), 7.73 (2H, d, $J = 8.4$ Hz), 8.11 (1H, dd, $J = 2.7$ Hz, $J = 8.4$ Hz), 8.39 (1H, d, $J = 2.7$ Hz), 8.47 (1H, dd, $J = 2.1$ Hz, $J = 4.8$ Hz), 8.74 (1H, s), 9.14 (1H, s, H-purine), 9.38 (1H, s, H-purine), 9.87 (1H, d, $J = 7.2$ Hz), 10.69 (1H, s, CONH), 13.19 (1H, s), 13.89 (1H, s, 9*H*-purine). ^{13}C NMR (75 MHz, DMSO-d_6): δ 114.19, 115.16, 118.88, 120.49, 120.89, 121.63, 123.80, 124.26, 124.87, 125.90 (q, CF_3), 129.01, 129.32, 131.83, 133.39, 137.79, 138.58, 141.75, 144.83, 149.53, 149.94, 151.37, 153.11, 153.25, 165.47 (CONH). IR (KBr, cm^{-1}): 3192, 3102, 2992, 2839, 1674, 1593, 1570, 1522, 858, 768.

*4.1.6.14. 3-((3-(9H-purin-6-yl)pyridin-2-yl)amino)-4-chloro-N-(3-(trifluoromethyl)phenyl)benzamide (**20l**).* Yellow solid (80 mg, 27.6%) was obtained from **13l**. Mp: 300–302 °C. HRMS (ESI^+) *m/z* calculated for $C_{24}H_{15}ClF_3N_7O$ $[M+H]^+$ 510.1051; found, 510.1055. ^1H NMR [300 MHz, DMSO-d_6]: δ 7.19 (1H, dd, $J = 4.8$ Hz, $J = 7.8$ Hz), 7.47 (1H, d, $J = 7.8$ Hz), 7.59–7.63 (2H, m), 7.73 (1H, d, $J = 8.1$ Hz), 8.05 (1H, d, $J = 8.1$ Hz), 8.27 (1H, s), 8.47 (1H, dd, $J = 1.8$ Hz, $J = 4.8$ Hz), 8.75 (1H, s, H-purine), 9.13 (1H, s, H-purine), 9.38 (1H, s, $J = 1.8$ Hz), 9.86 (1H, d, $J = 1.8$ Hz), 10.69 (1H, s, CONH), 13.18 (1H, s), 13.98 (1H, s, 9*H*-purine). ^{13}C NMR (75 MHz, DMSO-d_6): δ 114.19, 115.02, 116.40, 119.86, 120.47, 120.88, 123.05, 123.77, 125.22, 125.76, 128.91, 129.25, 129.55 (q, CF_3), 133.67, 137.81, 139.92, 141.78, 144.63, 149.43, 149.83, 151.45, 152.83, 153.29, 165.54 (CONH). IR (KBr, cm^{-1}): 3090, 2988, 2922, 2847, 1666, 1607, 1564, 1526, 1332, 924, 793.

*4.1.6.15. 3-((3-(9H-purin-6-yl)pyridin-2-yl)amino)-4-chloro-N-(3-isopropylphenyl)benzamide (**20m**).* Yellow solid (69 mg, 29.0%) was obtained from **13m**. Mp: 170–172 °C. HRMS (ESI^+) *m/z* calculated for $C_{26}H_{22}ClN_7O$ $[M+H]^+$ 484.1647; found, 484.1655. ^1H NMR [300 MHz, DMSO-d_6]: δ 1.23 (6H, d, $(CH_3)_2CH$, $J = 6.9$ Hz), 2.88–2.93 (1H, m, $(CH_3)_2CH$), 7.00 (1H, d, $J = 7.5$ Hz), 7.18 (1H, dd, $J = 4.8$ Hz, $J = 7.8$ Hz), 7.27 (1H, t, $J = 7.8$ Hz), 7.57–7.63 (2H, m), 7.67–7.70 (2H, m), 8.47 (1H, dd, $J = 1.8$ Hz, $J = 4.8$ Hz), 8.75 (1H, s), 9.14 (1H, s, H-purine), 9.32 (1H, s, H-purine), 9.86 (1H, d, $J = 7.5$ Hz), 10.23 (1H, s, CONH), 13.15 (1H, s), 13.89 (1H, s, 9*H*-purine). ^{13}C NMR (75 MHz, DMSO-d_6): δ 23.80 ($CH(CH_3)_2$), 33.48 ($CH(CH_3)_2$), 114.13, 115.12, 117.97, 118.33, 120.47, 120.92, 121.75, 125.41, 128.41, 128.90, 129.42, 134.35, 137.64, 139.05, 141.76, 144.90, 148.78, 149.59, 149.97, 151.39, 153.02, 153.30, 165.11 (NHCO). IR (KBr, cm^{-1}): 3192, 3088, 2963, 2868, 2835, 1653, 1603, 1576, 1526, 762, 702.

*4.1.6.16. 3-((3-(9H-purin-6-yl)pyridin-2-yl)amino)-4-chloro-N-(3,4-dichlorophenyl)benzamide (**20n**).* Yellow solid (76 mg, 32.4%) was obtained from **13n**. Mp: 322–323 °C. HRMS (ESI^+) *m/z* calculated for $C_{23}H_{14}Cl_3N_7O$ $[M+H]^+$ 510.0398; found, 510.0412. ^1H NMR [300 MHz, DMSO-d_6]: δ 7.18 (1H, dd, $J = 4.8$ Hz, $J = 7.8$ Hz), 7.56–7.64 (2H, m), 7.70–7.79 (2H, m), 8.18 (1H, d, $J = 2.4$ Hz), 8.46 (1H, dd, $J = 1.8$ Hz, $J = 4.8$ Hz), 8.75 (1H, s, H-purine), 9.13 (1H, s, H-purine), 9.37 (1H, d, $J = 1.8$ Hz), 9.85 (1H, s), 10.56 (1H, s, CONH), 13.18 (1H, s), 13.89 (1H, s, 9*H*-purine). ^{13}C NMR (75 MHz, DMSO-d_6): δ 114.20, 115.23, 120.20, 120.38, 120.94, 121.40, 125.10, 125.81, 129.07, 129.81, 130.48, 130.81, 133.60, 137.80, 139.20, 141.80, 145.01, 149.60, 150.01, 151.40, 152.99, 153.30, 160.55 (CONH). IR (KBr, cm^{-1}): 3335, 3092, 2986, 2824, 1659, 1578, 1522, 827, 762.

*4.1.6.17. 3-((3-(9H-purin-6-yl)pyridin-2-yl)amino)-N-(4-chloro-3-(trifluoromethyl)phenyl)-4-fluorobenzamide (**20o**).* Yellow solid (91 mg, 39.3%) was obtained from **13o**. Mp: 319–321 °C. HRMS (ESI^+) *m/z* calculated for $C_{24}H_{14}ClF_4N_7O$ $[M+H]^+$ 528.0957; found, 528.0960. ^1H NMR [300 MHz, DMSO-d_6]: δ 7.08 (1H, dd, $J = 4.8$ Hz, $J = 7.8$ Hz), 7.43 (1H, dd, $J = 2.1$ Hz, $J = 8.4$ Hz), 7.63–7.66 (2H, m), 8.07–8.11 (1H, m), 8.37–8.38 (2H, m), 8.68 (1H, d, $J = 4.8$ Hz), 8.96 (1H, s, H-purine), 9.23 (1H, s, H-purine), 9.80 (1H, d, $J = 7.8$ Hz), 10.61 (1H, s, CONH), 12.88 (1H, s), 13.89 (1H, s, 9*H*-purine). ^{13}C NMR (75 MHz, DMSO-d_6): δ 113.73, 114.37, 114.70 ($J = 7.0$ Hz), 118.79 (q, CF_3), 121.21 ($J = 8.1$ Hz), 124.11, 124.54, 124.75, 126.32, 126.73, 128.90, 129.01, 129.42, 130.66, 131.79, 138.68, 141.64, 144.94, 149.59 ($J = 6.7$ Hz), 151.44, 153.15 ($J = 5.3$ Hz), 153.46, 156.48, 165.42 (NHCO). IR (KBr, cm^{-1}): 3192, 3102, 2992, 2839, 1674, 1593, 1570, 1522, 858, 768.

*4.1.6.18. N-(3-((3-(9H-purin-6-yl)pyridin-2-yl)amino)phenyl)-4-chloro-3-(trifluoromethyl)benzamide (**21a**).* Yellow solid (75 mg, 30.4%) was obtained from **16a**. Mp: 306–308 °C. HRMS (ESI^+) *m/z* calculated for $C_{24}H_{15}ClF_3N_7O$ $[M+H]^+$ 510.1051; found, 510.1056. ^1H NMR [300 MHz, DMSO-d_6]: δ 7.03 (1H, dd, $J = 4.8$ Hz, $J = 7.8$ Hz), 7.32 (1H, t, $J = 7.8$ Hz), 7.46 (1H, d, $J = 7.8$ Hz), 7.56 (1H, d, $J = 7.8$ Hz), 7.92 (1H, d, $J = 8.7$ Hz), 8.24 (1H, s), 8.27 (1H, dd, $J = 2.1$ Hz, 8.7 Hz), 8.37 (1H, dd, $J = 1.8$ Hz, $J = 4.8$ Hz), 8.40 (1H, d, $J = 1.8$ Hz), 8.69 (1H, s, H-purine), 9.09 (1H, s, H-purine), 9.76 (1H, d, $J = 7.8$ Hz), 10.51 (1H, s, NHCO), 12.55 (1H, s), 13.82 (1H, s, 9*H*-purine). ^{13}C NMR (75 MHz, DMSO-d_6): δ 112.42, 112.92, 113.92, 114.46, 116.22, 121.56, 123.73, 127.01 (q, CF_3), 128.68, 129.42, 131.75, 133.30. 133.80, 134.18, 138.96, 140.79, 141.68, 144.63, 149.78, 150.02, 152.07, 152.98, 153.94, 163.03 (NHCO).

*4.1.6.19. N-(3-((3-(9H-purin-6-yl)pyridin-2-yl)amino)-4-methylphenyl)-4-chloro-3-(trifluoromethyl)benzamide (**21b**).* Yellow solid (71 mg, 28.0%) was obtained from **16b**. Mp: 304–305 °C. HRMS (ESI^+) *m/z* calculated for $C_{25}H_{17}ClF_3N_7O$ $[M+H]^+$ 524.1208; found, 524.1211. ^1H NMR [300 MHz, DMSO-d_6]: δ 2.54 (3H, s, $ArCH_3$), 7.07 (1H, dd, $J = 4.8$ Hz, $J = 7.8$ Hz), 7.45 (1H, d, $J = 9.0$ Hz), 7.59 (1H, d, $J = 9.0$ Hz), 7.71 (1H, d, $J = 9.0$ Hz), 8.12 (1H, dd, $J = 2.4$ Hz, $J = 9.0$ Hz), 8.36–8.39 (2H, m), 8.73 (1H, s), 8.94 (1H, s, H-purine), 9.10 (1H, s, H-purine), 9.85 (1H, s), 10.56 (1H, s, NHCO), 12.45 (1H, s), 13.86 (1H, s, 9*H*-purine). ^{13}C NMR (75 MHz, DMSO-d_6): δ 18.75 (CH_3), 113.15, 113.75 (d, $J = 2.9$ Hz), 114.93, 123.94, 124.77, 127.00 (q, CF_3), 129.37, 129.89, 131.69, 132.28, 133.26, 133.65, 134.26, 136.61, 138.84, 139.11, 139.29, 141.70, 144.74, 149.83, 152.03, 153.08, 154.16, 166.18 (NHCO).

*4.1.6.20. N-(3-((3-(9H-purin-6-yl)pyridin-2-yl)amino)-4-methylphenyl)-3-(trifluoromethyl)benzamide (**21c**).* Yellow solid

(50 mg, 20.6%) was obtained from **16c**. Mp: 293–294 °C. HRMS (ESI^+) *m/z* calculated for $C_{25}H_{18}F_3N_7O$ $[M+H]^+$ 490.1598; found, 490.1591. ^1H NMR [300 MHz, DMSO-d_6]: δ 2.44 (3H, s, $ArCH_3$), 7.03 (1H, dd, *J* = 4.8 Hz, *J* = 7.8 Hz), 7.25 (1H, d, *J* = 8.1 Hz), 7.47 (1H, d, *J* = 8.1 Hz), 7.81 (1H, t, *J* = 7.8 Hz), 7.96 (1H, d, *J* = 7.8 Hz), 8.27–8.36 (3H, m), 8.67 (1H, d, *J* = 1.6 Hz), 8.71 (1H, s), 9.08 (1H, s, H-purine), 9.79 (1H, s), 10.42 (1H, s, CONH), 12.29 (1H, s), 13.83 (1H, s, 9*H*-purine). ^{13}C NMR (75 MHz, DMSO-d_6): δ 18.26 (CH_3), 113.08, 113.69, 113.94, 115.00, 120.73, 122.89, 123.90, 124.24 (d, *J* = 2.3 Hz), 125.06, 127.23, 127.82, 129.10 (q, CF_3), 129.86, 131.76, 135.95, 136.78, 139.07, 141.69, 144.55, 149.87 (d, *J* = 3.7 Hz), 152.12, 152.94, 154.22, 163.76 (NHCO).

*4.1.6.21. N-(3-((3-(9H-purin-6-yl)pyridin-2-yl)amino)-4-methylphenyl)-3-cyanobenzamide (**21d**).* Yellow solid (76 mg, 34.1%) was obtained from **16d**. Mp: 303–305 °C. HRMS (ESI^+) *m/z* calculated for $C_{25}H_{18}N_8O$ $[M+H]^+$ 447.1676; found, 447.1680. ^1H NMR [300 MHz, DMSO-d_6]: δ 2.50 (3H, s, $ArCH_3$), 7.04 (1H, dd, *J* = 4.8 Hz, *J* = 7.8 Hz), 7.25 (1H, d, *J* = 8.1 Hz), 7.49 (1H, dd, *J* = 2.1 Hz, *J* = 8.1 Hz), 7.75 (1H, t, *J* = 7.8 Hz), 8.04–8.07 (1H, m), 8.26–8.28 (1H, m), 8.36 (1H, dd, *J* = 2.1 Hz, *J* = 4.8 Hz), 8.43 (1H, d, *J* = 1.5 Hz), 8.68 (1H, d, *J* = 2.1 Hz), 8.72 (1H, s, H-purine), 9.09 (1H, s, H-purine), 9.82 (1H, s), 10.38 (1H, s, NHCO), 12.32 (1H, s), 13.85 (1H, s, 9*H*-purine). ^{13}C NMR (75 MHz, DMSO-d_6): δ 18.31 (CH_3), 111.39, 113.07, 113.57, 113.75, 114.68, 118.33 (CN), 123.79, 129.55, 129.64, 129.90, 131.25, 132.48, 134.71, 136.03, 136.74, 139.05, 141.70, 144.61, 149.86, 149.92, 152.06, 152.98, 154.15, 163.33 (NHCO).

*4.1.6.22. N-(3-((3-(9H-purin-6-yl)pyridin-2-yl)amino)-4-methylphenyl)-4-chloro-3-methylbenzamide (**21e**).* White-off solid (84 mg, 35.7%) was obtained from **16e**. Mp: 301–302 °C. HRMS (ESI^+) *m/z* calculated for $C_{25}H_{20}ClN_7O$ $[M+H]^+$ 470.1491; found, 470.1490. ^1H NMR [300 MHz, DMSO-d_6]: δ 2.21 (3H, s, $ArCH_3$), 2.34 (3H, s, $ArCH_3$), 7.25 (1H, d, *J* = 8.4 Hz), 7.49 (1H, dd, *J* = 2.1 Hz, *J* = 8.4 Hz), 7.56 (1H, d, *J* = 7.8 Hz), 8.06 (1H, d, *J* = 7.8 Hz), 8.27 (1H, dd, *J* = 2.1 Hz, *J* = 4.8 Hz), 8.36 (1H, dd, *J* = 2.1 Hz, *J* = 4.8 Hz), 8.43 (1H, d, *J* = 1.8 Hz), 8.68 (1H, d, *J* = 1.8 Hz), 8.72 (1H, s, H-purine), 9.08 (1H, s, H-purine), 9.80 (1H, s), 10.38 (1H, s, NHCO), 12.32 (1H, s), 13.85 (1H, s, 9*H*-purine). ^{13}C NMR (75 MHz, DMSO-d_6): δ 17.67 (CH_3), 19.83 (CH_3), 113.56, 114.02, 119.39, 120.48, 121.06, 122.65, 127.31, 128.74, 129.44, 129.91, 131.94, 132.85, 135.29, 138.21, 139.14, 141.72, 144.64, 149.90, 149.94, 151.98, 152.98, 154.13, 165.80 (NHCO).

*4.1.6.23. N-(3-((3-(9H-purin-6-yl)pyridin-2-yl)amino)-4-methylphenyl)-3-chlorobenzamide (**21f**).* Yellow solid (93 mg, 39.5%) was obtained from **16f**. Mp: 311–313 °C. HRMS (ESI^+) *m/z* calculated for $C_{24}H_{18}ClN_7O$ $[M+H]^+$ 456.1334; found, 456.1331. ^1H NMR [300 MHz, DMSO-d_6]: δ 2.43 (3H, s, $ArCH_3$), 7.04 (1H, dd, *J* = 4.8 Hz, *J* = 7.8 Hz), 7.24 (1H, d, *J* = 8.4 Hz), 7.47 (1H, dd, *J* = 2.1 Hz, *J* = 9.0 Hz), 7.57 (1H, t, *J* = 8.4 Hz), 7.66 (1H, d, *J* = 9.0 Hz), 7.94 (1H, d, *J* = 7.8 Hz), 8.03 (1H, d, *J* = 1.8 Hz), 8.36 (1H, dd, *J* = 2.1 Hz, *J* = 4.8 Hz), 8.67 (1H, d, *J* = 1.8 Hz), 8.72 (1H, s, H-purine), 9.09 (1H, s, H-purine), 9.82 (1H, s), 10.30 (1H, s, NHCO), 12.30 (1H, s), 13.84 (1H, s, 9*H*-purine). ^{13}C NMR (75 MHz, DMSO-d_6): δ 18.79 (CH_3), 113.53, 114.24, 114.29, 115.34, 124.29, 126.95, 127.88, 129.88, 130.36, 130.74, 131.64, 133.60, 137.35, 137.52, 139.48, 142.20, 145.17, 150.41, 150.46, 152.60, 153.35, 154.69, 164.44 (NHCO).

*4.1.6.24. N-(3-((3-(9H-purin-6-yl)pyridin-2-yl)amino)-4-methylphenyl)-3-methoxybenzamide (**21g**).* Yellow solid (100 mg, 44.4%) was obtained from **16g**. Mp: 275–277 °C. HRMS (ESI^+) *m/z* calculated for $C_{25}H_{21}N_7O_2$ $[M+H]^+$ 452.1839; found, 452.1838. ^1H NMR [300 MHz, DMSO-d_6]: δ 2.43 (3H, s, $ArCH_3$), 3.81 (3H, s, CH_3O), 7.03 (1H, dd, *J* = 4.8 Hz, *J* = 7.8 Hz), 7.15 (1H, dd, *J* = 1.6 Hz, *J* = 8.1 Hz), 7.22 (1H, d, *J* = 8.7 Hz), 7.44 (2H, t, *J* = 7.8 Hz), 7.50–7.57 (2H, m), 8.35 (1H, dd, *J* = 2.1 Hz, *J* = 4.8 Hz), 8.64 (1H, d, *J* = 2.1 Hz), 8.71 (1H, s, H-purine), 9.08 (1H, s, H-purine), 9.80 (1H, s), 10.02 (1H, s, CONH), 12.27 (1H, s), 13.83 (1H, s, 9*H*-purine). ^{13}C NMR (75 MHz, DMSO-d_6): δ 18.27 (CH_3), 55.27 (OCH_3), 112.81, 112.98, 113.69, 114.03, 115.02, 117.14, 119.85, 123.71, 129.42, 129.39, 129.82, 136.48, 137.06, 138.93, 141.68, 144.66, 149.94, 149.98, 152.13, 153.03, 154.24, 159.10, 164.98 (NHCO).

*4.1.6.25. N-(3-((3-(9H-purin-6-yl)pyridin-2-yl)amino)-4-methylphenyl)-3-(dimethylamino)benzamide (**21h**).* Yellow solid (70 mg, 31.0%) was obtained from **16h**. Mp: 242–245 °C. HRMS (ESI^+) *m/z* calculated for $C_{26}H_{24}N_8O$ $[M+H]^+$ 465.2146; found, 465.2145. ^1H NMR [300 MHz, DMSO-d_6]: δ 2.42 (3H, s, $ArCH_3$), 3.00 (6H, s, $(CH_3)_2N$), 6.90–6.93 (1H, m), 7.02 (1H, dd, *J* = 4.8 Hz, *J* = 7.8 Hz), 7.20–7.33 (4H, m), 7.43 (1H, dd, *J* = 2.1 Hz, *J* = 8.1 Hz), 8.34 (1H, dd, *J* = 2.1 Hz, *J* = 4.8 Hz), 8.61 (1H, d, *J* = 2.1 Hz), 8.71 (1H, s, H-purine), 9.08 (1H, s, H-purine), 9.82 (1H, dd, *J* = 2.1 Hz, *J* = 7.8 Hz), 10.05 (1H, s, CONH), 12.26 (1H, s), 13.85 (1H, s, 9*H*-purine). ^{13}C NMR (75 MHz, DMSO-d_6): δ 18.26 (CH_3), 40.09 ($N(CH_3)_2$), 111.24, 112.95, 113.67, 114.18, 115.04, 115.13, 115.23, 123.63, 128.75, 129.63, 129.78, 135.82, 137.28, 138.88, 141.68, 144.67, 149.98, 149.99, 150.22, 152.14, 152.98, 154.28, 165.94 (NHCO).

4.2. In vitro B-Raf^{V600E} kinase assay

Activity of full length B-Raf^{V600E} was determined using HotSpot^{SM} kinase assay which was performed by Reaction Biology Corp. (Malvern PA). 5 nM of human GST-tagged B-Raf^{V600E} protein (AA416-766) (Invitrogen, Cat# PV3849) was mixed with 20 μM of the substrate His6-Tagged Full-length Human MEK1 (K97R) (Reaction Biology Corp.) in reaction buffer (20 mM Hepes pH 7.5, 10 mM $MgCl_2$, 1 mM EGTA, 0.02% Brij35, 0.02 mg/mL BSA, 0.1 mM Na_3VO_4, 2 mM DTT, 1% DMSO) at room temperature, then compounds dissolved in 100% DMSO at indicated doses (starting at 30 μM with 3-fold dilution) was delivered into the kinase reaction mixture by Acoustic technology (Echo550; nanoliter range), incubate for 20 min at room temperature. After 10 μM ^{33}P-γ-ATP (specific activity 10 μCi/μL) (P-ERKin Elmer, NEG302H001 MC) was added to initiate the reaction, the reactions were carried out at 25 °C for 120 min. The kinase activities were detected by filter-binding method. IC_{50} values and curve fits were obtained by Prism (GraphPad Software).

4.3. Antiproliferative assay in A375 cell lines in vitro

EnoGeneCell™ Counting Kit-8 (Cologne, Germany) was used to evaluate the inhibition effect on the growth of Human A375 melanoma cells. After diluting to 5×10^4 cells mL^{-1} with the complete medium, 100 μL of human A375 melanoma cells suspension was added to each well of 96-well culture plates and cultured in DMEM/10% fetal bovine serum for 24 h, with 5% CO_2 water saturated atmosphere at 37 °C. The synthesized compounds, Sorafenib and Verumrafenib were initially prepared at 20 mM in DMSO. Aliquots (200 μL) were diluted into 20 mL culture medium giving 200 μM, and prepared into 10 doses with two-fold dilutions. Aliquots (100 μL) of each dilution were added to the wells, giving doses ranging from 0.196 μM to 100 μM. A negative control group and vehicle control group each were also set. After further incubated at 37 °C for another 72 h in a humidified atmosphere with 5% CO_2, the cell viability was assessed by CCK-8 treatment and carried out strictly according to the manufacturer instructions (EnoGeneCell). The absorbance at 450 nm was recorded using MK3 Thermo microplate reader. Then IC_{50} values were calculated using GraphPad Prism 5 Software.

4.4. p-ERK cellular assay in A375 cells and SK-MEL-2 cells

A375 and SK-MEL-2 human melanoma cell line were both obtained from American Type Culture Collection (Manassas, VA). A375 cells were seeded at 0.15×10^6 cells/well into 24 well plates in DMEM medium and SK-MEL-2 cells were grown in EMEM medium supplemented with 10% heat-inactivated fetal bovine serum (FBS), 100 μg/mL penicillin, and 100 μg/mL streptomycin. The cells were treated with compounds or DMSO for 90 min. The final DMSO concentration for each culture sample was 0.5%. After treatment, the culture medium was removed and the cells were washed once with ice cold PBS. 60 μL of SDS sample buffer (62.5 mM Tris–HCl pH 6.8, 2% SDS, 10% Glycerol, 0.01% bromophenol red, 50 mM DTT) was added to each well of the 24 well plates to lyse the cells. The lysed cell samples were transferred to eppendorf tubes. The samples were then sheared using 27 gauge needles to shear DNA in the whole cell lysates. 15 μL of cell lysate samples were separated by SDS-PAGE with 10% Bis-Tris gel and transferred onto nitrocellulose membranes by iBlot dry blotting system (Life Technologies).

The membranes were blocked with 3% non-fat milk for 2 h and probed with primary anti-phospho-ERK1/2 antibody for overnight. Alexa Fluor633 goat anti rabbit IgG was used to detect the primary antibody. The membranes were scanned by Typhoon 9410 (GE Healthcare Life Sciences, Pittsburgh, PA). The blots were then stripped with a stripping buffer (100 mM Glycine, pH 2.5, 200 mM NaCl, 0.1% Tween 20 and 0.1% beta-mercaptoethanol) and reprobed with anti-ERK1/2 antibody and the Alexa Fluor633 goat anti rabbit IgG secondary antibody to get the ERK protein expression signal for each sample. In some cases, separate gels were run and the blots were probed anti-ERK1/2 antibody directly. The specific signals of bands of interest were quantified by Gel-Pro Analyzer. The IC_{50} values of the testing compounds were calculated using the GraphPad Prism 5 program based on a sigmoidal dose–response equation.

4.5. In vivo A375 xenograft assay protocol in Balb/c-nu nude mice

Adult female Balb/c-nu nude mice (4–6 weeks of age and 16–17 g of weight) were purchased from Shanghai Sciple-Rubicam experimental animals Ltd. with License Number of SCXK (Shanghai) 2008–0016, housed in SPF animal facility with a 12-h light/dark cycle, and provided with rodent chow and tap water adlibitum. All animal care and experimental procedures were reviewed and approved by our Institutional Animal Care and Use Committee. Human melanoma A375 cells were purchased from ATCC. Cells were expanded in culture at 37 °C humidified atmosphere containing 5% CO_2 using DMEM supplemented with 10% fetal bovine serum (Gibco). All cells were kept in culture for less than 10 passages. Cells growing at 80% confluence were harvested for implantation using 0.25% trypsin and re-suspended in PBS at a concentration of 5×10^7 cells/mL. 100 μL of cell suspension was injected subcutaneously. When tumor volume reached approximately 100 mm^3, mice were randomized into groups. The compounds were dissolved in vehicle (Cremophor EL (Sigma):95% medicinal ethanol:water = 1.25:1.25:7.5) affording a concentration of 5 mg/mL. The compound solution and vehicle were intragastrically administered into each group, respectively, once daily for 23 days. The mice body weights and the diameters of tumors were measured twice a week. To the end of the experiment, mice were dissected to obtain the weight of the tumor.

Acknowledgments

This work was financially supported by the Fundamental Research Funds for the Central Universities (No. JKZ2011005), Youth project of National Natural Science Foundation of China (No. 81102318/H3001) and A Project Funded by the Priority Academic Program Development of Jiangsu Higher Education Institutions. We also express our gratitude to Dr. Yuren Wang, Dr. Jianghong Wu and Dr. Jamie Planck (Reaction Biology Corporation, Pennsylvania, USA) for their helpful support in biological evaluation.

Abbreviations

MAPK	mitogen-activated protein kinase
MEK	mitogen-activated protein kinase kinase
ERK	extracellular signal-regulated kinase
V600E	a substitution of a glutamic acid for valine at residue 600
DFG	a conserved amino acid sequence of D594 F595 and G596
wt	wild-type
FDA	Food and Drug Administration
SAR	structure–activity relationships
EDCI	1-ethyl-3-(3-dimethylaminopropyl)carbodiimide hydrochloride
HOBt	*N*-hydroxybenzotriazole
DMF	*N*,*N*-dimethylformamide
THF	tetrahydrofuran
$PdCl_2$(dppf)	1,1′-bis-(diphenylphosphino)ferrocene-palladium(II) dichloride
LiHMDS	lithium hexamethyldisilazide
EtOAc	ethyl acetate
THP	tetrahydropyran
TsOH	*p*-toluenesulfonic acid
ESI	electrospray ionization
HRMS	high-resolution mass spectroscopy
±SD	standard deviation
±SEM	standard error of the mean
TLC	thin-layer chromatography
DMSO	dimethyl sulfoxide
FBS	fetal bovine serum
DMEM	Dulbecco's modified eagle medium
SD	solid dispersion

Appendix A. Supplementary data

Supplementary data related to this article can be found at http://dx.doi.org/10.1016/j.ejmech.2014.10.039.

References

[1] C. Peyssonnaux, A. Eychene, The Raf/MEK/ERK pathway: new concepts of activation, Biol. Cell 93 (2001) 53–62.
[2] H.F. Li, Y.D. Chen, S.S. Rao, X.M. Chen, H.C. Liu, J.H. Qin, W.F. Tang, Y. Wang, X.F. Zhou, T. Lu, Recent advances in the research and development of B-Raf inhibitors, Curr. Med. Chem. 17 (2010) 1618–1634.
[3] P.T.C. Wan, M.J. Garnett, S.M. Roe, S. Lee, D. Niculescu-Duvaz, V.M. Good, C.M. Jones, C.J. Marshall, C.J. Springer, D. Barford, R. Marais, Mechanism of activation of the RAF-ERK signaling pathway by oncogenic mutations of B-RAF, Cell 116 (2004) 855–867.
[4] J. Cohen, M.Z. Xing, E. Mambo, Z.M. Guo, G.G. Wu, B. Trink, U. Beller, W.H. Westra, P.W. Ladenson, D. Sidransky, BRAF mutation in papillary thyroid carcinoma, J. Natl. Cancer Inst. 95 (2003) 625–627.
[5] C. Sawyers, Targeted cancer therapy, Nature 432 (2004) 294–297.
[6] H.B. El-Nassan, Recent progress in the identification of BRAF inhibitors as anti-cancer agents, Eur. J. Med. Chem. 72 (2014) 170–205.
[7] W.M. Yang, Y.D. Chen, Y.M. Zhang, S.Z. Tang, H.L. Chen, W.F. Tang, T. Lu, Design, synthesis and antitumor activities of bis-arylureas and bis-arylamides based on 1H-benzo[d]imidazole moiety as novel b-Raf(V600E)/VEGFR2 dual inhibitors, Lett. Drug Des. Discov. 11 (2014) 1079–1089.
[8] P.B. Chapman, A. Hauschild, C. Robert, J.B. Haanen, P. Ascierto, J. Larkin, R. Dummer, C. Garbe, A. Testori, M. Maio, D. Hogg, P. Lorigan, C. Lebbe, T. Jouary, D. Schadendorf, A. Ribas, S.J. O'Day, J.A. Sosman, J.M. Kirkwood, A.M.M. Eggermont, B. Dreno, K. Nolop, J. Li, B. Nelson, J. Hou, R.J. Lee, K.T. Flaherty, G.A. McArthur, Improved survival with Vemurafenib in melanoma with BRAFV600E mutation, N. Engl. J. Med. 364 (2011) 2507–2516.

[9] A. Hauschild, J.J. Grob, L.V. Demidov, T. Jouary, R. Gutzmer, M. Millward, P. Rutkowski, C.U. Blank, W.H. Miller, E. Kaempgen, S. Martin-Algarra, B. Karaszewska, C. Mauch, V. Chiarion-Sileni, A.M. Martin, S. Swann, P. Haney, B. Mirakhur, M.E. Guckert, V. Goodman, P.B. Chapman, Dabrafenib in BRAF-mutated metastatic melanoma: a multicentre, open-label, phase 3 randomised controlled trial, Lancet 380 (2012) 358–365.
[10] K.T. Flaherty, I. Puzanov, K.B. Kim, A. Ribas, G.A. McArthur, J.A. Sosman, P.J. O'Dwyer, R.J. Lee, J.F. Grippo, K. Nolop, P.B. Chapman, Inhibition of mutated, activated BRAF in metastatic melanoma, N. Engl. J. Med. 363 (2010) 809–819.
[11] R.M. Anforth, T.C.M.P. Blumetti, R.F. Kefford, R. Sharma, R.A. Scolyer, S. Kossard, G.V. Long, P. Fernandez-Penas, Cutaneous manifestations of dabrafenib (GSK2118436): a selective inhibitor of mutant BRAF in patients with metastatic melanoma, Brit. J. Dermatol. 167 (2012) 1153–1160.
[12] G.S. Falchook, G.V. Long, R. Kurzrock, K.B. Kim, T.H. Arkenau, M.P. Brown, O. Hamid, J.R. Infante, M. Millward, A.C. Pavlick, S.J. O'Day, S.C. Blackman, C.M. Curtis, P. Lebowitz, B. Ma, D. Ouellet, R.F. Kefford, Dabrafenib in patients with melanoma, untreated brain metastases, and other solid tumours: a phase 1 dose-escalation trial, Lancet 379 (2012) 1893–1901.
[13] P.I. Poulikakos, C. Zhang, G. Bollag, K.M. Shokat, N. Rosen, RAF inhibitors transactivate RAF dimers and ERK signalling in cells with wild-type BRAF, Nature 464 (2010) 427–430.
[14] F. Su, A. Viros, C. Milagre, K. Trunzer, G. Bollag, O. Spleiss, J.S. Reis, X.J. Kong, R.C. Koya, K.T. Flaherty, P.B. Chapman, M.J. Kim, R. Hayward, M. Martin, H. Yang, Q.Q. Wang, H. Hilton, J.S. Hang, J. Noe, M. Lambros, F. Geyer, N. Dhomen, I. Niculescu-Duvaz, A. Zambon, D. Niculescu-Duvaz, N. Preece, L. Robert, N.J. Otte, S. Mok, D. Kee, Y. Ma, C. Zhang, G. Habets, E.A. Burton, B. Wong, H. Nguyen, M. Kockx, L. Andries, B. Lestini, K.B. Nolop, R.J. Lee, A.K. Joe, J.L. Troy, R. Gonzalez, T.E. Hutson, I. Puzanov, B. Chmielowski, C.J. Springer, G.A. McArthur, J.A. Sosman, R.S. Lo, A. Ribas, R. Marais, RAS mutations in cutaneous squamous-cell carcinomas in patients treated with BRAF inhibitors, N. Engl. J. Med. 366 (2012) 207–215.
[15] M. Okaniwa, M. Hirose, T. Arita, M. Yabuki, A. Nakamura, T. Takagi, T. Kawamoto, N. Uchiyama, A. Sumita, S. Tsutsumi, T. Tottori, Y. Inui, B.C. Sang, J. Yano, K. Aertgeerts, S. Yoshida, T. Ishikawa, Discovery of a selective kinase inhibitor (TAK-632) targeting pan-RAF inhibition: design, synthesis, and biological evaluation of C-7-substituted 1,3-benzothiazole derivatives, J. Med. Chem. 56 (2013) 6478–6494.
[16] E.K. Shim, N.D. Kim, T.B. Shim, S.Y. Kim, Novel purinylpyridinylamino-2,4-difluorophenyl sulfonamide derivative, pharmaceutically acceptable salt thereof, preparation method thereof, and pharmaceutical composition with inhibitory activity against raf kinase, containing same as active ingredient, PCT Int. Appl., WO2012074249 A2 (2012) 81.
[17] W.K. Choi, M.I. El-Gamal, H.S. Choi, D. Baek, C.H. Oh, New diarylureas and diarylamides containing 1,3,4-triarylpyrazole scaffold: synthesis, antiproliferative evaluation against melanoma cell lines, ERK kinase inhibition, and molecular docking studies, Eur. J. Med. Chem. 46 (2011) 5754–5762.
[18] A. Gopalsamy, G. Ciszewski, Y. Hu, F. Lee, L. Feldberg, E. Frommer, S. Kim, K. Collins, D. Wojciechowicz, R. Mallon, Identification of pyrazolo[1,5-a]pyrimidine-3-carboxylates as B-Raf kinase inhibitors, Bioorg. Med. Chem. Lett. 19 (2009) 2735–2738.
[19] J. Tang, K.E. Lackey, S.H. Dickerson, The discovery of potent and selective 4-aminothienopyridines as B-Raf kinase inhibitors, Bioorg. Med. Chem. Lett. 23 (2013) 66–70.
[20] J. Dietrich, V. Gokhale, X. Wang, L.H. Hurley, G.A. Flynn, Application of a novel [3+2] cycloaddition reaction to prepare substituted imidazoles and their use in the design of potent DFG-out allosteric B-Raf inhibitors, Bioorg. Med. Chem. 18 (2010) 292–304.
[21] R.K. Robins, E.F. Godefroi, E.C. Taylor, L.R. Lewis, A. Jackson, Purine nucleosides. I. The synthesis of certain 6-substituted-9-(tetrahydro-2-pyrany1)-purines as models of purine deoxynucleosides, J. Am. Chem. Soc. 83 (1961) 2574–2579.
[22] J.B. Press, R. Falotico, Z.G. Hajos, R.A. Sawyers, R.M. Kanojia, L. Williams, B. Haertlein, J.A. Kauffman, C. Lakas-Weiss, J.J. Salata, Synthesis and SAR of 6-substituted purine derivatives as novel selective positive inotropes, J. Med. Chem. 35 (1992) 4509–4515.
[23] M.M. Vasbinder, B. Aquila, M. Augustin, H. Chen, T. Cheung, D. Cook, L. Drew, B.P. Fauber, S. Glossop, M. Grondine, E. Hennessy, J. Johannes, S. Lee, P. Lyne, M. Mortl, C. Omer, S. Palakurthi, T. Pontz, J. Read, L. Sha, M. Shen, S. Steinbacher, H. Wang, A. Wu, M. Ye, Discovery and optimization of a novel series of potent mutant B-Raf(V600E) selective kinase inhibitors, J. Med. Chem. 56 (2013) 1996–2015.
[24] S.M. Soond, P.A. Townsend, S.P. Barry, R.A. Knight, D.S. Latchman, A. Stephanou, ERK and the F-box protein betaTRCP target STAT1 for degradation, J. Biol. Chem. 283 (2008) 16077–16083.